IEEE Access
Multidisciplinary ⋮ Rapid Review ⋮ Open Access Journal

Received 11 September 2023, accepted 3 October 2023, date of publication 9 October 2023, date of current version 12 October 2023.

Digital Object Identifier 10.1109/ACCESS.2023.3322930

RESEARCH ARTICLE

AquaHet-PSO: An Informative Path Planner for a Fleet of Autonomous Surface Vehicles With Heterogeneous Sensing Capabilities Based on Multi-Objective PSO

MICAELA JARA TEN KATHEN[1], FEDERICO PERALTA SAMANIEGO[1], ISABEL JURADO FLORES[1], AND DANIEL GUTIÉRREZ REINA[2]

[1]Departamento de Ingeniería, Universidad Loyola Andalucía, 41704 Seville, Spain
[2]Departamento de Ingeniería Electrónica, Universidad de Sevilla, 41092 Seville, Spain

Corresponding author: Micaela Jara Ten Kathen (mcjaratenkathen@al.uloyola.es)

This work has been partially funded by the Ministerio de Ciencia e Innovación under the Projects "AQUATRONIC (Ref. Codes: PID2021-126921OA-C22 and PID2021-126921OB-C21)" and "ECOPORT (Ref. Codes: TED2021-131326A-C22 and TED2021-131326B-C21)".

ABSTRACT The importance of monitoring and evaluating the quality of water resources has significantly grown over time. To achieve this effectively, an option is to employ an intelligent monitoring system capable of measuring the physical and chemical parameters of water. Surface vehicles equipped with sensors for measuring water quality parameters offer a viable solution for these missions. This work presents a novel approach called AquaHet-PSO, which addresses the challenge of simultaneously monitoring multiple water quality parameters with several peaks of contamination using a heterogeneous fleet of autonomous surface vehicles. Each vehicle in the fleet possesses a different set of sensors, such as number of sensors and sensor types, which is the definition provided by the authors for a heterogeneous fleet. The AquaHet-PSO consists of three main phases. In the initial phase, the vehicles traverse the water resource to obtain preliminary models of water quality parameters. These models are then utilized in the second phase to identify potential contamination areas and assign vehicles to specific action zones. In the final phase, the vehicles focus on a comprehensive characterization of the parameters. The proposed system combines several techniques, including Particle Swarm Optimization and Gaussian Processes, with the integration of genetic algorithm to maximize the distances between the initial positions of vehicles equipped with identical sensors, and a distributed communication system in the final phase of the AquaHet-PSO. Simulation results in the Ypacarai lake demonstrate the effectiveness and efficiency of AquaHet-PSO in generating accurate water quality models and detecting contamination peaks. The proposed method demonstrated improvements compared to the lawnmower approach. It achieved a remarkable 17% improvement, on r-squared data, in generating complete models of water quality parameters throughout the lake. In addition, it achieved a 230% improvement in accurate characterization of high pollution areas and a 24% increase in pollution peak detection specifically for heterogeneous fleets equipped with four or more identical sensors.

INDEX TERMS Autonomous surface vehicle, Gaussian process, genetic algorithm, heterogeneous fleet, informative path planning, multi-objective problem, particle swarm optimization, water resource monitoring.

The associate editor coordinating the review of this manuscript and approving it for publication was Diego Oliva.

NOMENCLATURE

$\mathcal{P}$	Set of vehicles in the fleet.
$p \in \mathcal{P}$	A vehicle.
$\mathcal{S}$	Set of measurable water quality parameters by the fleet.
$s \in \mathcal{S}$	A water quality parameter sensor.
$\mathcal{S}_{(p)} \subseteq \mathcal{S}$	Subset of sensors of vehicle p.
$\mathcal{N} \subset \mathbb{R}^2$	Set of coordinates within a 2D space.
$\mathbf{x} \in \mathcal{N}$	$= (x, y)$ A location, coordinate.
$\mathcal{Q} \subset \mathcal{N}$	Set of coordinates where the fleet measured water quality values.
$\mathcal{Q}_{(p)} \subseteq \mathcal{Q}$	Subset of the coordinates where water quality was measured by the ASV p.
$\mathcal{Q}_{(s)} \subseteq \mathcal{Q}$	Subset of the coordinates where the water quality parameter s was measured by any of the ASVs in the fleet.
$\mathcal{U} \subset \mathcal{N}$	Set of all coordinates where any of the ASVs in the fleet where located.
$\mathcal{U}_{(p)} \subseteq \mathcal{U}$	Subset of the coordinates through which the ASV p passed.
$\mathcal{A} \subset \mathcal{N}$	Set of all action zones.
$\mathcal{A}_{(s)} \subseteq \mathcal{A}$	Subset of all action zones of the water quality parameter s.
$\mathcal{Z} \subset \mathcal{N}$	Set of all combined action zones.
$z \in \mathcal{Z}$	A combined action zone.
$\mathcal{P}_{(z)} \subseteq \mathcal{P}$	Subset of the vehicles assigned to the combined action zone z.
$\mathcal{S}_{(z)} \subseteq \mathcal{S}$	Subset of sensors of combined action zone z.
$y_s(\mathbf{x})$	Ground truth value of the water quality parameter s at location $\mathbf{x}$.
$\hat{y}_s(\mathbf{x})$	Estimated model value of the water quality parameter s at location $\mathbf{x}$.
K	Covariance (kernel) matrix of the Gaussian Process.
$\mu_s(\mathbf{x})$	Mean value estimated by a Gaussian Process of the water quality parameter s at location $\mathbf{x}$.
$\sigma_s(\mathbf{x})$	Uncertainty value obtained by a Gaussian Process of the water quality parameter s at location $\mathbf{x}$.
t	Time

I. INTRODUCTION

The importance of maintaining healthy water environments is evident. Animals and plants depend on water to live. Therefore, the more healthy a water body is, the more it will help to balance its ecosystem. However, human waste and bad practices pollute water bodies such as lakes and lagoons, due to industrial and agricultural activities [1]. Then, the water ecosystem fails to be balanced, generally creating excess of nutrients such as nitrates and phosphorus, which leads to the proliferation of a green-blue algae, which is a toxic algae that drains oxygen and kills life inside the water [2]. This *eutrophization* problem can be found all around the world including China, Sri Lanka, Paraguay and the United States [3], [4], [5].

To efficiently overcome this problem, government agencies and research centers must develop plans to treat water bodies or to maintain a certain water quality level. Both of which can be highly inefficient if the lake or river is not monitored periodically considering these *water quality levels* [6]. Water quality can be described with a set of physico-chemical parameters of water, including potential of Hydrogen, dissolved oxygen, total of dissolved solids. The knowledge of the values of these Water Quality Parameters (WQPs) can help for either treating water or maintaining water quality on a certain level. Therefore, monitoring such parameters is a crucial task in this situation.

Current efforts for water quality monitoring include fixed stations, manual measurement campaigns and monitoring through the usage of Autonomous Surface Vehicles (ASVs) [7]. The first method consists of chemical laboratories installed on the shore of lakes, that continuously measure on a specific location within the water body. The second improves the general knowledge by manually obtaining samples from different locations and then returning these samples to a laboratory for a post-process evaluation. The latter presents a mixture of both of the former methods because a vehicle can travel to any location within a particular enclosed water body and additionally can be teleoperated, which decreases the exposure of probable toxic waters to humans. Additionally, if the vehicles are equipped with electronic water quality sensors, measurements can be performed in real time and water quality can be obtained during the monitoring mission. Moreover, these values can help for decision making strategies regarding the location of measurement, providing a more efficient usage of resources. The relative cost of monitoring through Autonomous Surface Vehicles (ASVs) is considering to be cheaper than the other methods and can provide better results. Monitoring with ASVs can be efficient because water WQPs patterns can vary on a weekly basis [8], and this type of monitoring is relatively quick, minimizing the likelihood of significant changes in the WQPs.

ASVs are composed of modules that have different functions in order to fulfill the task of monitoring water resources. These modules can be seen in Fig. 1. The perception module allows the ASV to know its environment and where it is positioned. The ASV sensors are located in this module. Some of the papers related to this module are those presented in [9] and [10]. The learning module is composed of a surrogate model that uses the data from the perception module to generate a models of the environment, the number of models depends on the number of WQPs to be measured. These models are used in the planning module to calculate an optimized informative path to solve a specific problem, as demonstrated in the work by [11]. Finally, the control module and the ASV dynamics are in charge of the ASV movement, i.e. their function is to make the ASV go to the points assigned by the informative path planner. Some advances in this area can be found in [12]. The informative path planner approach incorporates real-time measurements

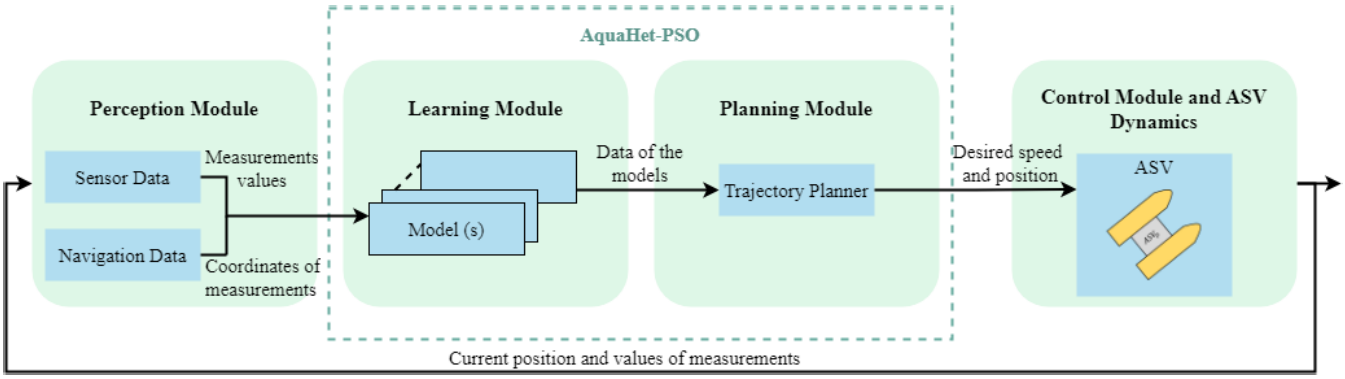

FIGURE 1. Block diagram of the proposed monitoring system: AquaHet-PSO.

of water quality parameters into the calculation of the next vehicle position, taking advantage of available environmental information [13].

This work focuses on the learning and planning modules. It is considered that multiple WQPs need to be monitored simultaneously, and also that there are multiple ASVs available. The monitoring mission focuses on obtaining the models of the WQPs and on finding peaks of contamination or pollution (that can be described as an optimization problem) within a large-scale lake scenario. In that sense, an intelligent online informative path planning framework is proposed to solve the problem at hand. Furthermore, the considered fleet of ASVs have different sensors available, so that an heterogeneous optimization system must be designed to fully accomplish the monitoring mission. The problem can be described as a multi-objective optimization, in which the agents in charge of obtaining values within a search or decision space can only evaluate some of the objectives. We propose a Multi-objective Particle Swarm Optimization (PSO) technique designed for an heterogeneous fleet of ASVs. The PSO algorithm was chosen based on a comparative study conducted in [14],where various Swarm Intelligence (SI) algorithms were evaluated. The results of this comparison indicated that PSO offers several advantages for monitoring application. Specifically, it is known for its ease of implementation and minimal requirement for initial parameters. Consequently, the PSO was selected as the foundational algorithm for the proposed informative path planning approach. The system is in charge of obtaining informative paths that considers the properties of ASVs as well as the lake scenario (water quality map models). The proposed system is called AquaHet-PSO, due to the heterogeneous design of a PSO for aquatic vehicles, and is composed of three main operational phases: exploration, resource allocation, and exploitation. The exploration phase focuses on the generation of initial WQPs models. In the resource allocation phase, ASVs are allocated to areas with high levels of contamination identified in the initial models, the combined action zones. Finally, in the exploitation phase, the system exploits the contamination zones in order to characterize in depth the areas with high levels of contamination. During the exploitation phase, the AquaHet-PSO system incorporates the distributed learning technique to ensure the autonomy of the ASV sub-fleet deploying in the combined action zones. The heterogeneous nature of ASVs, with different number and types of sensors, poses a challenge in determining their initial positioning. ASVs equipped with identical sensors starting from relatively close positions can hinder effective surface exploration of water resources due to inadequate separation between vehicles. For this reason, the Genetic Algorithm (GA) is employed to maximize the distance between the initial positions of ASVs with the same measurement capabilities, namely sensors of the same type. In summary, our proposal introduces a novel concept by addressing a scenario where ASVs in a fleet have different sensor capabilities, i.e. different number and type of WQP sensors. This diversity gives rise to a multi-objective problem: creating accurate models for all WQPs. To achieve this, ASVs, taking into account the unique configurations of their sensors, must have the ability to identify the optimal positions for measurements. This is where AquaHet-PSO plays a key role. It generates real-time trajectories for each ASV, guiding them to collect measurements at optimal positions, taking into account all sensors onboard each ASV. This innovative approach enables efficient and comprehensive water quality monitoring in a variety of environments. The AquaHet-PSO contributes substantially on monitoring and informative path planning, as well as in the framework that has been designed and is proposed in this work. The contribution can be summarized as follows:

1) The development of a monitoring system based on multi-objective multi-modal particle swarm optimization and Gaussian processes for a heterogeneous fleet of autonomous surface vehicles capable of generating accurate models of water quality parameters and detecting areas with high levels of contamination in real time.
2) The optimization of the initial positioning of ASVs equipped with sensors that measure the same water quality parameter by utilizing a genetic algorithm.
3) The application of the proposed monitoring system in the case of the Ypacarai lake, showing the effectiveness

of the proposed system over a multi-objective and heterogeneous lawnmower.

The following sections describes the literature review in Section II, followed by the statement of the problem in Section III. Next, Section IV described the AquaHet-PSO, thoroughly. An implementation of the proposed system can be found in Section V, including results for a simulation setup. The work is concluded in Section VI, with a mentioning of future works.

II. RELATED WORK

Current efforts regarding the mentioned problem can be grouped into three different groups: i) Monitoring approaches, ii) Usage of ASVs and iii) PSO techniques. Monitoring approaches consider ASVs as well as other types of vehicles including Aerial and Ground vehicles. For example, the authors in [15] describe a monitoring mission for crops using aerial vehicles using a Gaussian Process-based approach, in which different parameters are measured from different heights using onboard sensors. In [16], the authors introduce a novel path planner employing Evolutionary Algorithms (EA) for an ASV. This planner seeks to optimize the ASV trajectory and to obtain information about the distribution of cyanobacteria in water currents and the cyanobacteria behavior during the mission. In [17], the authors propose an innovative approach, an adaptive visual information gathering (AVIG) framework, for Autonomous Underwater Vehicles (AUVs) exploring benthic environments. This framework incorporates Decision-time Adaptive Replanning (DAR), Sparse Gaussian Process (SGP), and Convolutional Neural Network (CNN) techniques to dynamically adapt the exploration of the robot based on real-time visual data obtained from the environment. On the other hand, in [18], an heterogeneous system (aerial and ground vehicles) mission is proposed to explore and monitor a defined region using active exploration algorithms for detecting radiation locations with the aerial drone and performing extensive information acquisition with the ground vehicle. Heterogeneous vehicle systems consists of using vehicles with different capabilities that works towards achieving to the same goal [19]. They are mainly used to exploit the different advantages that each type of vehicle can contribute. Heterogeneous systems have also been studied, in [20], where a cell wall based paradigm was proposed to optimize the throughput of heterogeneous aerial vehicles networking. A multi-agent system was proposed in [21], where the multiple heterogeneous aerial agents aimed to cover a large area for network resource orchestration based on virtual networks. Another approach [22] proposed the usage of aerial vehicles with communication constraints that constructed coverage paths in a multi-robot patrolling mission scenario. The mentioned work used coordination techniques that efficiently utilized information from multiple sources to update their paths. More recently, Zhang et al. [23] proposed the usage of underwater vehicles to obtain information about a sea floor through the usage of cooperative coverage path planning mechanisms based on dot-spreading definition and visiting. Definitely, (homogeneous and heterogeneous) autonomous vehicles where used for the monitoring mission.

Specifically to monitoring water quality, recent works include [14], [24] and [25]. These works start from the premise that a exploration is needed to obtain good, reliable WQP model. Most of the related work use ASVs to perform monitoring since they are reusable, safe and reliable for the task at hand. Moreover, there exists a set of works that propose monitoring systems for the Ypacarai Lake. Such is the case of Arzamendia et al. [26] that used as a basis the Genetic Algorithm (GA) to solve the lake monitoring problem. The problem was modeled as the Traveling Salesman Problem (TSP) and the objective is to cover the largest possible area of the water resource. To meet this objective, the authors determined beacons on the shores of the lake where the ASV should pass. The same authors propose a modification in [27], where the problem is modeled with the Chinese Postman Problem (CPP). This improvement allows the ASVs to visit the beacons more than once, maximizing the coverage area of the monitoring system. It is remarkable that none of the mentioned system regarding monitoring using ASVs considers that the ASVs can be heterogeneous in the sense of the available water quality sensors, despite that this decision can only improve economic resources, since not every vehicle will have the same number of water quality sensors.

Finally, regarding PSO techniques, in [28], the authors introduce a heterogeneous fleet comprising an underwater vehicle, a surface vehicle, and an aerial vehicle for conducting underwater target tracking missions. The system is divided into two phases: the initial search for the target location and the subsequent tracking phase. To address the problem of path planning in the presence of obstacles, an improved PSO is employed in the second phase. Wang et al. [29] developed multiple path planning approaches utilizing the distributed-PSO algorithm to address the path planning challenges faced by a swarm of UAVs. These planners designed for conducting reconnaissance missions. The authors in [30] introduce a novel approach that combines the PSO algorithm with the Model Predictive Control (MPC) technique. By integrating the PSO with the MPC, they propose a cooperative control strategy for planning path and tracking trajectories designed for intelligent vehicles. In [31], the authors integrate PSO with Reinforcement Learning (RL) to solve multi-objective problems, the MCMOPSO-RL (Multi-Objective Particle Swarm Optimization with Multi-Mode Collaboration based on Reinforcement Learning). MCMOPSO-RL is a path planner that combines PSO and RL techniques to optimize trajectories while simultaneously taking into account multiple objectives and constraints.

A brief summary of the related work regarding monitoring techniques is shown in Table 1, where the third column describes the main approach of each proposed strategy. The definition of heterogeneity varies among the authors mentioned in this section. Some authors consider fleets

TABLE 1. Brief summary of the related work.

Publication	Year	Main Approach	Heterogeneous
[15]	2022	Online mapping.	No
[16]	2023	Cyanobacteria monitoring.	No
[17]	2021	Underwater environment exploration.	No
[18]	2019	Detection of radiation locations.	Aerial and ground vehicles.
[19]	2021	Coverage path planning.	Characteristics of AUVs.
[20]	2021	Optimization of vehicle network performance.	UAS swarm networking.
[21]	2021	Area coverage.	Network resources.
[22]	2013	Coverage path planning.	Characteristics of AUVs.
[23]	2021	Coverage path planning.	Characteristics of AUVs.
[24]	2021	WQPs monitoring and estimation.	No
[14]	2021	WQPs monitoring and estimation.	No
[25]	2022	WQPs monitoring and estimation.	No
[26]	2019	WQPs monitoring.	No
[27]	2019	WQPs monitoring.	No
[28]	2022	Search and tracking mission.	Aerial, surface and underwater vehicles.
[29]	2019	Reconnaissance missions.	No
[30]	2020	Path planning and trajectory tracking.	No
[31]	2022	Trajectory optimization.	No

as heterogeneous when the vehicles are of different types (ASVs, UAVs, etc.), while others define heterogeneity based on varying characteristics such as speed or energy levels. Therefore, the Heterogeneous column provides clarification on what the authors refer to as heterogeneous fleets.

The works discussed in this section serve as a basis for comparison, but a direct comparison is not possible because, according to the authors, AquaHet-PSO is the first system to consider vehicles that do not have the same types of sensors onboard simultaneously. The authors define a heterogeneous fleet as a group of ASVs equipped with different types of sensors, which may not necessarily match the sensors on other ASVs. The combination of these approaches and techniques offers several clear advantages: online route generation for multi-objective monitoring, the ability to generate models of water quality parameters and detect contamination peaks using a heterogeneous fleet, and broader coverage of the water resource by optimizing initial positions through GA.

III. PROBLEM MODELLING AND SYSTEM ARCHITECTURE

A. PROBLEM MODELLING

The ASV fleet consists of P vehicles, that do not necessarily share the same water quality sensing capabilities, hence a heterogeneous system. The ASVs have several sensors capable of measuring different water quality parameters s, each sensor measuring one parameter. As ASVs are heterogeneous, the vehicles do not have the same type of sensor on board. The proposed informative path planner uses the measurements taken for each WQP to calculate the next position to which the ASVs should go. This translates to a multi-objective problem, since, by having multiple WQPs, the planner must consider multiple criteria to obtain the best position to which the ASVs should travel.

The main objective is to minimize the error between the actual states of the water quality parameters s represented by ground truths $y_s(\mathbf{x})$ and the models estimated with the proposed monitoring system $\hat{y}_s(\mathbf{x})$, subject to a maximum Euclidean distance max_dist that the ASVs can travel, Eq. 1.

$$\begin{aligned} min \quad & f(\mathbf{x}) = \frac{1}{S}\sum_{s=1}^{S} f_s(\mathbf{x}) \\ s.t. \quad & \frac{1}{P}\sum_{p=1}^{P} dist\_ASV_p \leq max\_dist \end{aligned} \tag{1}$$

The function $f_s(\mathbf{x})$ is the Mean Square Error (MSE) between the actual state of the water quality parameters $y_s(\mathbf{x})$ and the model estimated $\hat{y}_s(\mathbf{x})$ as shown in Eq. 2. The term $\mathbf{x}$ refers to the coordinate (x, y) on the surface of the water resource, this term is being discretized to N points within the search space. The term S refers to the total number of WQP sensors that are measured.

$$f_s(\mathbf{x}) = \frac{1}{N}\sum_{i=1}^{N}(y_s(\mathbf{x}_i) - \hat{y}_s(\mathbf{x}_i))^2 \tag{2}$$

The monitoring system is carried out in water resources. Therefore, the search space is the entire surface of the water resource. The search space is represented by a matrix $\mathcal{M}$ of $n \times m$, where each element of the matrix $\mathcal{M}_{ij}$ has a dimension of $d \times d$ and has a value. The value of $\mathcal{M}_{ij}$ represents the state of the element: 1) if the value is equal to 0, ASVs cannot to travel to that grid, since it represents an obstacle, land or forbidden zone; 2) if the value is equal to 1, the grid is available for ASVs to travel through. All available grid coordinates are in the set $\mathcal{N}$.

B. SYSTEM ARCHITECTURE

The system architecture of the proposed approach comprises three main parts: i) the ASVs, ii) the water quality sensors, and iii) the global coordinator. These parts are explained below:

- **ASV:** The set of sensors owned by each ASV is not necessarily the same as the set of sensors on board of other ASVs. Therefore, regarding the available sensors, the ASVs are heterogeneous. At the start of the mission, all ASVs have the same energy level. The monitoring task ends when the average distance traveled by the ASVs is equal to max_dist. It is assumed that the battery of the ASVs has enough autonomy to finish the monitoring task. Since the movements of the ASVs are synchronized, all vehicles end the monitoring tasks at the same time.

The ASVs are equipped with a robust obstacle avoidance system, often implemented using computer vision techniques. Additionally, they are outfitted with a sonar system capable of measuring the depth of the surrounding environment. This feature enables the ASVs to identify shallow areas and effectively steer clear of them, enhancing navigation safety. Furthermore, the ASVs are equipped with a differential Global Positioning System (GPS) that operates in tandem with a base station. This comprehensive set of sensors and systems empowers ASVs to navigate complex water bodies, avoid obstacles, and maintain accurate positioning.

- **Sensors:** The sensors employed for measuring WQPs are assumed to be in an ideal state. This signifies that the sensors are regarded as well-calibrated and functioning accurately as the monitoring tasks are initiated. These sensors measure discretely, at a position $\mathbf{x}$ where an ASV is located. The locations where the measurements were taken conform the $\mathcal{Q} \subset \mathcal{N}$ set.
  The locations where the pth vehicle has measured corresponds to a subset

$$\mathcal{Q}_{(p)} = \{\mathbf{x} \in \mathcal{Q} \mid \mathbf{x} \text{ measured by vehicle } p\} \quad (3)$$

  Thorough this paper the subindex (p) will be used to denote subsets that are relevant only to the pth vehicle.
  During the monitoring process, the sensor data is transformed into a normalized range between 0 and 1. Additionally, to categorize the water quality status, three levels are considered. The first level represents an acceptable status and ranges from 0 to 33%. The second level indicates a warning level and ranges from 34 to 66%. The last level signifies a risk level and ranges from 67 to 100%. These thresholds are determined based on the maximum contamination value measured. The specific value of 33% was chosen by the authors to ensure that each level encompasses a similar range of values.
  Communication between the ASV system and the WQPs sensors is established through a USB connection.
- **Global coordinator:** The global coordinator is located in the cloud, and the ASVs are connected to it via 4G technology. Communication between the ASVs is done through the centralized system. Communication solely occurs between the vehicles and the central server; there is no inter-vehicle communication. Data from the sensors are sent to the cloud and they are used to generate the responses of the data model in the global coordinator.
  An illustration of the communications between the parts of the proposed monitoring system is shown in Fig. 2.

IV. PROPOSED INFORMATIVE PATH PLANNER: AQUAHET-PSO

The proposed approach is a multi-modal, multi-objective monitoring system that has the ability to process data and generate models for several water quality parameters $s_1, s_2, \ldots, s_S$, the AquaHet-PSO. The AquaHet-PSO is a monitoring system that combines the components of the PSO, the GP data, and the GA. In the proposed monitoring system, the ASV fleet consists of vehicles with diverse measurement capabilities. This means that the vehicles are equipped with different types and quantities of sensors.

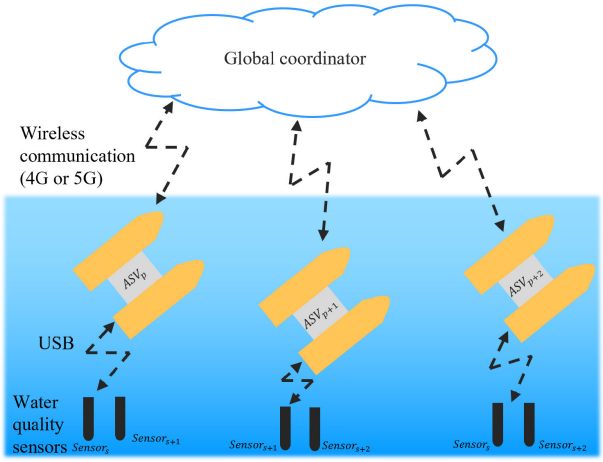

FIGURE 2. Communication between the global coordinator, the ASVs and the sensors.

A. CLASSICAL PARTICLE SWARM OPTIMIZATION

The PSO, developed by [32], is an optimization algorithm based on the social behavior of flocks of birds and school of fish. This algorithm allows working with several individuals simultaneously. The individuals are called particles and represent possible solutions to an optimization problem, a set of particles is called swarm. The movement of the particles is based on a control component, an auto-cognitive component or local best, and a social cognitive component or global best. The local best is the best position of the particle up to the moment where the term is calculated. In contrast to the local best, the global best is the best position of the swarm up to the moment where the term is calculated. The expressions for calculating the velocity $\mathbf{v}^{t+1}$ and the position $\mathbf{x}^{t+1}$ of the particle p are shown below:

$$\mathbf{v}_p^{t+1} = \omega \mathbf{v}_p^t + c_1 r_1^t \left[\mathbf{pbest}_p^t - \mathbf{x}_p^t\right] + c_2 r_2^t \left[\mathbf{gbest}^t - \mathbf{x}_p^t\right] \quad (4a)$$

$$\mathbf{x}_p^{t+1} = \mathbf{x}_p^t + \mathbf{v}_p^{t+1} \quad (4b)$$

the ω term is the control parameter or the inertia weight, the local best of the particle p at time t is represented by the term $\mathbf{pbest}_p^t$, the $\mathbf{gbest}^t$ term is the global best of the swarm at time t. To determine the importance of the auto-cognitive and social component of the PSO, the algorithm has two weights c_1 and c_2, also called acceleration coefficients. r_1 and r_2 are two random values between 0 and 1.

B. GAUSSIAN PROCESS

Gaussian Processes (GP) are probabilistic machine learning models based on Bayesian inference [33]. The GP input data are considered random variables and the output a multivariate

Gaussian distribution. The behavior of the GP is defined by two functions: i) the covariance function or kernel function, and ii) the mean function. Usually, the mean function is zero for convenience.

The GP input data are the measurements taken from the water resource $y_s(\mathbf{x}) : \mathbf{x} \in \mathcal{Q}$ and the $\mathcal{Q}$ set. For the GP Regression update, these data are marginalized and conditioned. The unknown responses $(\mu(\mathbf{x}_*), \sigma(\mathbf{x}_*))$ of the GPR $(\hat{y}(\mathbf{x})_*)$ are obtained by applying the equations shown below:

$$\mu_s(\mathbf{x}_*) = K_*^T (K + \sigma_o^2)^{-1} \hat{y}_s(\mathbf{x}) \tag{5a}$$

$$\sigma_s(\mathbf{x}_*) = K_{**} - K_*^T (K + \sigma_o^2)^{-1} K_* \tag{5b}$$

The term σ_o represents the expected measurement noise in the context of GP modeling. This parameter plays a crucial role in refining water quality measurements obtained through GPs, as it allows for a more accurate adjustment of the data [11]. The terms K, K_{**} and K_* are obtained from the fitted kernel. These terms include covariances between known data $k(\mathbf{x}, \mathbf{x})$ and unknown data $k(\mathbf{x}*, \mathbf{x}*)$, as well as covariances between both the known and unknown data $k(\mathbf{x}, \mathbf{x}*)$.

$$\begin{aligned} K &= \begin{bmatrix} K & K_* \\ K_*^T & K_{**} \end{bmatrix} = \begin{bmatrix} k(\mathbf{x}, \mathbf{x}) & k(\mathbf{x}, \mathbf{x}*) \\ k(\mathbf{x}*, \mathbf{x}) & k(\mathbf{x}*, \mathbf{x}*) \end{bmatrix} \\ &\mathbf{x} : \mathbf{x} \in \mathcal{Q} \\ &\mathbf{x}* : \mathbf{x}* \in \mathcal{N} \end{aligned} \tag{6}$$

The estimate of water quality parameters $\hat{y}(\mathbf{x})$ at any location $\mathbf{x}$ is obtained from the GP mean. Therefore, for the following sections, mention is made of $\mu_s(\mathbf{x})$ as the model estimated by the monitoring system. The standard deviation or uncertainty of the model is $\sigma_s(\mathbf{x})$.

C. INITIAL POSITIONS

In a multi-objective problem where ASVs share at least one sensor, the initial positions of the ASVs play a crucial role. The farther apart the ASVs with shared sensors are, the larger the area they can collectively cover. However, in the AquaHet-PSO, the ASVs are heterogeneous, which makes determining the optimal starting positions a complex task. Since a Gaussian Process model is fitted according to the measurements, the farther apart these measurements are, the better (so that to reduce the model uncertainty). However, the initial distribution of sensors across the search space is dependent on the vehicles themselves, so an initial allocation of the vehicles need to be done. To address this, a Genetic Algorithm (GA) is employed to assign the starting points of the ASVs. The initial positioning problem of the ASVs is considered an NP-hard problem due to the large number of possible solutions resulting from the various permutations of initial positions that each vehicle could occupy.

Using a set of specific points $\mathbf{x}$ such as ports or clearings along the edge of the water resource as potential starting locations, a Genetic Algorithm searches for the optimal initial placement or location of the allotted vehicles. The specific objective in this stage is to maximize the distance between water quality sensors, ensuring that the vehicles are positioned as far apart as possible. This approach aims to optimize the initial coverage area and enhance the efficiency of data collection and monitoring.

The GA, influenced by the theory of evolution of Darwin, is a stochastic population-based algorithm [34]. Each solution is represented as a chromosome consisting of genes that encode specific parameters [35]. The GA employs various techniques such as selection, crossover, and mutation to simulate the natural process of evolution. These techniques help in improving the fitness of the population over successive generations, ultimately leading to the identification of an optimal solution [35]. For a more detailed explanation of the functioning of the GA, readers are referred to [34], [35], and [36]. Since the initial ports are predefined locations, these locations are encoded into an ordered list and the GA algorithm considers an individual as an specific subset of locations (according to the number of available vehicles). The list can be seen in Fig. 3. An example is shown in Fig. 4(b), where 8 vehicles must be located along a list of 8 possible locations. Each individual then contains the indices of the candidate starting locations and are defined as lists of indices. Using this approach, many classical operators can be used as they are since the individual or chromosome definition are identical to the classical individuals for a TSP problem found in several works [34], [35], [36].

The important difference with the general TSP approach is that the fitness function is not defined to minimize the distance between selected locations but to maximize the distance between sensors. Fortunately, the distance between sensors can be obtained according to the set of sensors that are shared between vehicles. Recalling that $\mathcal{S}_{(p)} \subseteq \mathcal{S}$ is the subset of sensors available in the pth vehicle, we aim to maximize the distance between two vehicles p_i and p_j whenever they share a common type of sensor s. Moreover, if the vehicles p_i and p_j share more than one sensor, the fitness of the individual is better since there are more sensors that are far apart. This information is encoded as the cardinality, or number of elements, in the intersection of sensors between vehicle p_i and vehicle p_j. With a direct proportion for both cardinality and distance between vehicles, the fitness function for the individual x, i.e., the list of indices related to the initial positions, that needs to be maximized in this GA approach is:

$$f(x) = \sum_{i=1}^{|\mathcal{P}|-1} \sum_{j=i+1}^{|\mathcal{P}|} |\mathcal{S}_{(p_i)} \bigcap \mathcal{S}_{(p_j)}| \cdot dist(p_i, p_j) \tag{7}$$

Implying that $dist(\cdot)$ is the Euclidean distance between the vehicles p_i and p_j located at different harbors and ports. The crossover operator to be used is the classical Ordered, which creates offspring based on an initial subset of one parent and completes the offspring with the remaining genes of the second parent in the order that they are found. Regarding mutation, a random shuffle is performed

TABLE 2. On-board sensors of the vehicles in the example shown in Fig. 4.

Vehicle	Sensors	Vehicle	Sensors
p_1	s_1, s_2	p_5	s_2, s_3
p_2	s_1, s_3	p_6	s_2, s_4
p_3	s_1, s_4	p_7	s_3, s_4
p_4	s_1, s_2	p_8	s_3, s_4

Port ID	Pos_x	Pos_y
0	800	5600
1	3700	1600
2	7800	8100
3	7400	12400
4	2000	4000
5	3200	9200
6	6400	6000
7	5200	1000

Vehicle ID	p_1	p_2	p_3	p_4	p_5	p_6	p_7	p_8
Allotted Port	4	2	7	5	1	3	6	0

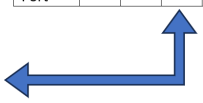

FIGURE 3. Example an individual for the initial location selection. In this example, vehicle p_3 must be initially located at position 7 (5200, 1000).

between pairs of genes, this is called the Shuffle Indices mutation operator. Tournament selection is used as well via a $\mu + \lambda$ GA approach [26]. Specific values for individual and population size and number of generations are set depending on the number of vehicles present in the current experiment. Additional values are defined in the experiments section.

Table 2 lists the sensors s owned by each vehicle p in an example of the monitoring task. Fig. 3 shows the chromosomes of the example in the process of maximizing the initial positions of the ASVs. The Port ID column refers to eight coordinate points of harbors and ports located around the Ypacarai lake. The selection of these coordinates was based on easily accessible locations or existing ports in the region. The objective of the new initial positioning of the ASVs is to generate the largest possible initial distance between vehicles equipped with the same type of sensor. In order to show an example in an illustrative way, Fig. 4 is presented. In the example shown in Fig. 4, the fitness of the initial positions without GA, Fig. 4(a), is 1386.79. However, the fitness of the maximized initial positions, Fig. 4(b), is 1581.79. This suggests an improvement in the initial disposition of the ASVs at the beginning of the mission.

D. INFORMATIVE PATH PLANNER

This subsection provides an explanation of the operational phases involved in the informative path planner, along with the process of measuring multiple WQPs. Initially, the procedures for calculating the components of the equations are presented. The equations governing the movements of ASVs in the exploration and exploitation phases are adaptations of the Enhanced GP-based PSO [14], Eq. 20a. Readers are encouraged to refer to Appendix A for further details and comprehensive information.

1) ENHANCED GP-BASED PSO COMPONENTS

The AquaHet-PSO is based on the Enhanced GP-based PSO algorithm [14] (Section A), dividing the monitoring mission into phases, where it first tries to cover the largest possible area of the water resource, then segments the area of the water resource and assigns ASVs to the zones to finally detect contamination peaks of different WQPs. The equations governing the speed and motion of the vehicles are equations based on the Enhanced GP-based PSO [14] and the studies conducted in [37] and [38]. Having different sensors, the ASV informative path planner must take into account multiple objectives to define the next position to travel. It should also be noted that there is no longer only one GP; on the contrary, a GP must be assigned for each WQP. These GPs are updated with the measured data of the water quality parameters $y_s(\mathbf{x}) : \mathbf{x} \in \mathcal{N}$ and the coordinates where the measurements were taken $\mathcal{Q}_{(s)} \subset \mathcal{Q}$. The subset $\mathcal{Q}_{(s)}$ is composed of the coordinates $\mathbf{x}$ where the measurements of the water quality parameters s were taken. To obtain the movement components, the proposed approach uses the data from the sensors owned by the ASV.

The movement components can be obtained by two different methods, i) the decoupled method, and ii) the coupled method. The methods are defined below:

a: DECOUPLED METHOD

This method is developed in order to give importance to one objective (water quality parameter) at a time and not simultaneously. However, during the monitoring task, different objectives are prioritized at different time periods. The multi-objective informative path planner selects, at a given time, the WQP that has the highest data value, obtains the coordinates where that data is located and the corresponding term is equal to that coordinate. Eq. 8 shows the equations to calculate the movement components.

$$\mathbf{pbest}_p^t(\mathbf{x}) = argmax\{\mu_s(\mathbf{x})\},\ s = [1, 2, .., S] : s \in \mathcal{S}_{(p)};\ \mathbf{x} \in \mathcal{U}_{(p)} \tag{8a}$$

$$\mathbf{gbest}_p^t(\mathbf{x}) = argmax\{\mu_s(\mathbf{x})\},\ s = [1, 2, .., S] : s \in \mathcal{S}_{(p)};\ \mathbf{x} \in \mathcal{U} \tag{8b}$$

$$\mathbf{max\_un}_p^t(\mathbf{x}) = argmax\{\sigma_s(\mathbf{x})\},\ s = [1, 2, .., S] : s \in \mathcal{S}_{(p)};\ \mathbf{x} \in \mathcal{N} \tag{8c}$$

$$\mathbf{max\_con}_p^t(\mathbf{x}) = argmax\{\mu_s(\mathbf{x})\},\ s = [1, 2, .., S] : s \in \mathcal{S}_{(p)};\ \mathbf{x} \in \mathcal{N} \tag{8d}$$

b: COUPLED METHOD

For this method, the linear scalarization is used. By applying linear scalarization, the multi-criteria problem becomes simple, since it transform a multi-objective problem into a single objective problem. Unlike the decoupled method, in this method all objectives (water quality parameters) are considered simultaneously. The equations for calculating the PSO components and the surrogate model data are shown in Eq. 9. These values are obtained from the argument of the maximum value of the sum of the mean of the models or the model uncertainty. In Eq. 9, the term w_{s_p} represents the importance given to each WQP. This weight is referred to as the sensor weight. The sensor weight will depend on the types of sensors s that the vehicle p has, $\mathcal{S}_{(p)}$, and the number of

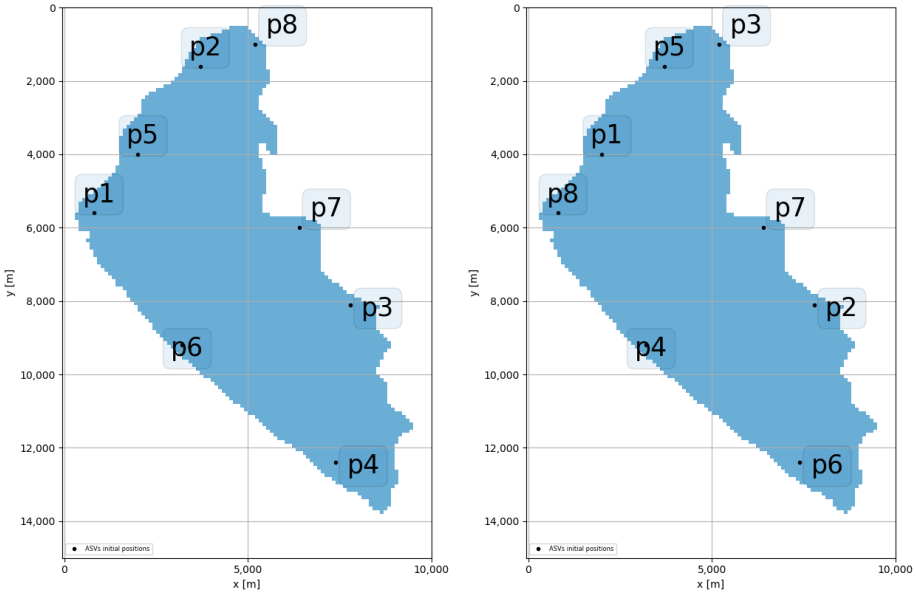

(a) Initial position of the ASVs without GA. (b) Initial position of the ASVs with GA.

FIGURE 4. Example of maximization of the initial position of the ASVs.

sensors of each parameter that the ASV fleets have. The more sensors of the same parameter, the lower the weight. This is defined with the objective of giving greater importance to the sensors that are in smaller quantity.

$$\mathbf{pbest}_p^t(\mathbf{x}) = argmax\{\sum_{s=1}^{S} w_{s\_p}\mu_s(\mathbf{x})\} : s \in \mathcal{S}_{(p)};\ \mathbf{x} \in \mathcal{U}_{(p)} \tag{9a}$$

$$\mathbf{gbest}_p^t(\mathbf{x}) = argmax\{\sum_{s=1}^{S} w_{s\_p}\mu_s(\mathbf{x})\} : s \in \mathcal{S}_{(p)};\ \mathbf{x} \in \mathcal{U} \tag{9b}$$

$$\mathbf{max\_un}_p^t(\mathbf{x}) = argmax\{\sum_{s=1}^{S} w_{s\_p}\sigma_s(\mathbf{x})\} : s \in \mathcal{S}_{(p)};\ \mathbf{x} \in \mathcal{N} \tag{9c}$$

$$\mathbf{max\_con}_p^t(\mathbf{x}) = argmax\{\sum_{s=1}^{S} w_{s\_p}\mu_s(\mathbf{x})\} : s \in \mathcal{S}_{(p)};\ \mathbf{x} \in \mathcal{N} \tag{9d}$$

As mention before, the weights depend on the types of sensors that each vehicle has. Since each vehicle can have different sensors, the sensor weights may vary from vehicle to vehicle. However, in all vehicles, the sum of the sensor weights complies with the condition shown below:

$$\sum_{s=1}^{S} w_{s\_p} = 1 \tag{10a}$$

$$\frac{1}{S_1}u + \frac{1}{S_2}u + \ldots + \frac{1}{S_S}u = 1 : s \in \mathcal{S}_{(p)} \tag{10b}$$

Each sensor weight is equal to one variable u divided by the total number of sensors S_s of the same type s in the entire fleet, Eq. 11. The sensors taken into account in this calculation are the ones owned by the ASV ($\mathcal{S}_{(p)}$). The value of u is obtained by clearing the variable from Eq. 10b. This value can vary between different ASVs. To obtain the weight of each sensor, Eq. 11 is applied after determining the value of u using Eq. 10.

$$w_{s\_p} = \frac{1}{S_s}u : s \in \mathcal{S}_{(p)} \tag{11a}$$

An example is shown below: considering a fleet with three ASVs ($|\mathcal{P}| = 3$), with the following sensor capabilities for each ASV: $\mathcal{S}_{(p1)} = \{s_1, s_2, s_3\}$, $\mathcal{S}_{(p2)} = \{s_1, s_3, s_4\}$, $\mathcal{S}_{(p3)} = \{s_4\}$. Therefore, the total amount of each type of sensor is: $S_1 = 2$, $S_2 = 1$, $S_3 = 2$, and $S_4 = 1$. To find the values of the sensor weights for each ASV, it is first necessary to find the value of u by applying the formulas in Eq. 10. After finding the value of u, the formula in Eq. 11 needs to be applied.

TABLE 3. Example of calculation of sensor weights.

p	u	w_1	w_2	w_3	w_4
1	0.5	0.25	0.5	0.25	0
2	0.67	0.33	0	0.33	0.33
3	1	0	0	0	1

The values of the weights for the example are presented in Table 3. In the case of p_1, as the number of s_2 sensors in the fleet is smaller, its weight is higher than the other sensors. On the other hand, p_2 has sensors with an equal number in the fleet, resulting in equal weight values. Lastly, p_3, having

only one sensor, has a weight value of 1 assigned to that sensor.

2) OPERATIONAL PHASES

The operational phases of the AquaHet-PSO is derived from the PSO and the GP, resulting in a monitoring mission that consists of three distinct phases: exploration, resource allocation, and exploitation. The exploration and exploitation phases play a crucial role in generating accurate models of the WQPs and detecting contamination zones in the proposed monitoring system. However, due to the heterogeneity of the fleet, where ASVs may have different types or quantities of sensors for measuring WQPs, efficient assignment of vehicles to specific areas becomes essential. Therefore, the resource allocation phase is a critical aspect of the proposed monitoring system.

a: EXPLORATION PHASE

The purpose of this phase is to obtain an initial model for different WQPs. To meet the objective, the ASVs must cover the largest possible surface area of the water body, i.e., explore the surface. In this first phase, the velocity of the ASVs are calculated using Eq. 12. The position is determined using the same equation as the Classic PSO, Eq. 4b.

$$\mathbf{v}_p^{t+1} = w\mathbf{v}_p^t + c_1 r_1^t[\mathbf{pbest}_p^t - \mathbf{x}_p^t] + c_3 r_3^t[\mathbf{max\_un}^t - \mathbf{x}_p^t] \tag{12}$$

The studies performed in [37] show that in order to have an optimal exploration, the global best **gbest** and maximum contamination **max_con** terms must be inactive. However, before calculating the velocity, a preliminary computation of the motion components is carried out, as described in Section IV-D1. The exploration phase ends when the vehicles have traveled a certain distance, this distance is called *exploration_distance* and represents a percentage of the maximum distance, *max_dist*, that the monitoring mission can last.

Algorithm 1 shows the pseudo-code of the exploration phase. Before starting the exploration task, the PSO must be initialized and the ground truth of the water quality parameters $\mathbf{y}_s$ must be created. In addition, the sensor weights must be calculated, and the ASVs must be assigned to the starting points by applying the GA. Then, the exploration phase begins. The local best $\mathbf{pbest}_p^t$ and global best $\mathbf{gbest}_p^t$ values are constantly calculated using Eq. 8a, 8b or Eq. 9a, 9b, depending on the selected method. When the ASVs reach a traveled distance l between the current position $\mathbf{x}^t$ and the last position where a measurement has been taken $\mathbf{x}_{measure}$, the sensors take a measurement. These measurements are used to update the GP of each WQP. The coordinates of the maximum contamination $\mathbf{max\_con}_p^t$ and maximum uncertainty $\mathbf{max\_un}_p^t$ are then calculated by applying Eq. 8d, 8c or Eq. 9d, 9c, depending on the selected method. Finally, the velocity $\mathbf{v}_p^{t+1}$ and next position $\mathbf{p}_p^{t+1}$ of the ASVs are calculated.

Algorithm 1 AquaHet-PSO Exploration Phase pseudo-Code

```
while dist ≤ exploration_distance do
    for pinP do
        pbest_p^t, gbest_p^t ← Obtain the values from Eq. 8 or Eq. 9*;
    dist ← x^t − x_measure ← Calculate distance
    if dist ≥ l then
        for pinP do
            for sinS_(p) do
                y_s(x) ← Take water resource measurements from the s parameter sensor
        for sinS do
            σ_s^t, μ_s^t ← Adjust the GP of the s parameter
        for pinP do
            max_un_p^t, max_con_p^t ← Obtain the values from Eq. 8 or Eq. 9*
    for pinP do
        v_p^{t+1}, x_p^{t+1} ← Update speed and position of the ASVs using Eq. 12 and Eq. 20b
```

*The terms $\mathbf{pbest}_p$, $\mathbf{gbest}_p$, $\mathbf{max\_un}_p$ and $\mathbf{max\_con}_p$ are calculated according to the selected method, coupled or decoupled.

b: RESOURCES ALLOCATION PHASE

The great challenge lies in the variety of parameters that must be measured, in addition to the fact that the ASVs do not have the same sensors. Consequently, the procedures must be adapted to solve multi-objective and heterogeneous monitoring problems. Therefore, the second phase of the system deals with the delimitation of potential pollution zones and the assignment of vehicles to these zones. In the following, the procedure is explained in detail.

- Combined Action Zones (CAZ): for the generation of the CAZ, the action zones must first be generated. To do this, using the model obtained in the exploration phase, the areas where contamination is high are located and action zones are generated. Action zones are circular areas of radius *rad* where water contamination values exceed a set threshold. The boundaries for the action zones are determined based on the levels of acceptable, warning, and risk, as described in Section III-B. For the generation of action zones, the warning and risk levels are taken into consideration. Therefore, any coordinate where the estimated water quality parameters (WQPs) fall within these levels is considered as part of an action zone. All action zones are located in set $\mathcal{A}$. However, action zones are determined for each specific WQP, which means that there can be several action zones in

total. The subset $\mathcal{A}_s \subset \mathcal{A}$ refers to the action zones pertaining to water quality parameters s.

Fig. 5(a) to Fig. 5(d) show examples of the generation of action zones of an s-sensor. Each circle represents an action zone created. The higher the *Priority* value of the zone, the higher the contamination levels of the zone. These zones have the function of limiting the surface area to be exploited by the ASVs with the objective of deepening the monitoring in these zones. Action zones do not overlap. If a coordinate has already been assigned to an action zone, it will no longer be considered for the other zones.

Due to the significant number of action zones, the AquaHet-PSO proceeds to create CAZ. The set $\mathcal{Z}$ is composed of all action zones combined. These CAZs are formed by merging overlapping action zones. We proposed a sequential procedure to generate the CAZ. It is important to highlight that the following steps or phases are not excluding. Therefore, the step 2 will be applied if with execution of the step 1 at least a vehicle is not assigned to each CAZ. The procedure is at follows:

- Step 1 - Prioritize heterogeneity: when CAZs are formed by merging overlapping action zones of different parameters, without considering overlaps of action zones for the same parameter. The overlapping of action zones belonging to the same WQP is not realized due to the heterogeneity of the fleet. This is because the presence of different sensors on board allows an ASV to exploit action zones of different sensors at the same time, allowing a more focused exploitation of two or more parameters in smaller areas. This approach differs from overlapping action zones of the same sensor, which would result in larger zones targeting a single WQP.

  This situation arises when the distance between the centers of action zones for different sensors is smaller than the combined sum of their respective action zone radii (distance between $center_{1_{s1}}$ and $center_{1_{s2}} > rad_{s1} + rad_{s2}$). However, an exception is made if an action zone of parameter s_n overlaps with two action zones of parameter s_{n+1}. An example of this is seen in the overlapping of the action zones between s_2 (Fig. 5(b)) and s_3 (Fig. 5(c)). The result is the convergence of these action zones into a single CAZ, as depicted in Fig. 5(e), CAZ 0. In addition, the operation of the step 1 can be seen in Fig. 5(e), which shows different areas where the action zones of the same sensor are not merged (orange-tinted areas in the lower margin of the figure and green-tinted areas in the upper left margin).
- Step 2 - Prioritize homogeneity: If after the application of step 1 there are still zones without ASVs assigned, new CAZs need to be generated. In step 2, the overlap between zones of the same sensor is also taken into account. This is because of the limited availability of ASVs and the potential for an ASV to exploit multiple zones of the same sensor. Fig. 5(f) shows the merging of the different action zones into 3 CAZs, where the zones corresponding to the same sensor are also overlapped.
- Step 3 - Enlarge coverage: based on the CAZs generated in step 2), if there is a zone to which no ASV is assigned, the radius of that zone is increased until it overlaps with another CAZ, thus ensuring an overlap of CAZs. This can be seen in Fig. 5(g), where no ASV was assigned in one of the CAZs.

These phases are determined based on the allocation of vehicles. Initially, CAZs are created following the conditions specified in phase 1. If there are any CAZs that are not assigned to a vehicle, the zones described in step 2 are generated. Vehicle assignment is then conducted, and if there are still CAZs remaining without assigned vehicles, the overlapping of CAZs (step 3) is generated. The subset $\mathcal{S}_z$ consists of the water quality parameters s to which the CAZs z belong. It is worth noting that although a different order can be followed for the previous steps of the CAZ generation, simulation results have conducted and the proposed order is the one that the best results achieved.

- Assignment of ASVs: the assignment of vehicles is carried out based on the sensors that each ASV possesses and the WQPs of the CAZs. After the generation of the CAZ, a scan is performed between the sensors of each ASV and the parameters of each CAZ. This enables determining the number of common sensors between them (*Priority*). As the values increase, so does the priority level. These data are utilized for resource allocation, where the ASV with the highest priority is the one that shares the most sensors in common with any CAZ. In cases where multiple CAZ have the same *Priority*, the decision criterion shifts to the number of potential vehicles that can be assigned to each zone, *Number of possibilities*. This number reflects the count of vehicles that share an equal number of sensors in common with the CAZ. The vehicle selected for assignment to the CAZ is the one with the lowest probability of being assigned to another CAZ, ensuring optimal distribution. This process continues until all the CAZ have an ASV assigned to them. Vehicles that are assigned to the CAZ z are located in subset $\mathcal{P}_{(z)}$ There are a couple of excluding scenarios that can arise:
  - Scenario 1: when there are more CAZs than available ASVs, the problem is resolved by regenerating the CAZs.
  - Scenario 2: when there are more vehicles than action zones, in such cases, the sensors possessed by each vehicle are considered, and the vehicle is assigned to the zone with the highest number of sensor matches. In cases where multiple CAZs have an equal number of sensors in common with the vehicle, the ASV is assigned to the zone with the largest surface area.

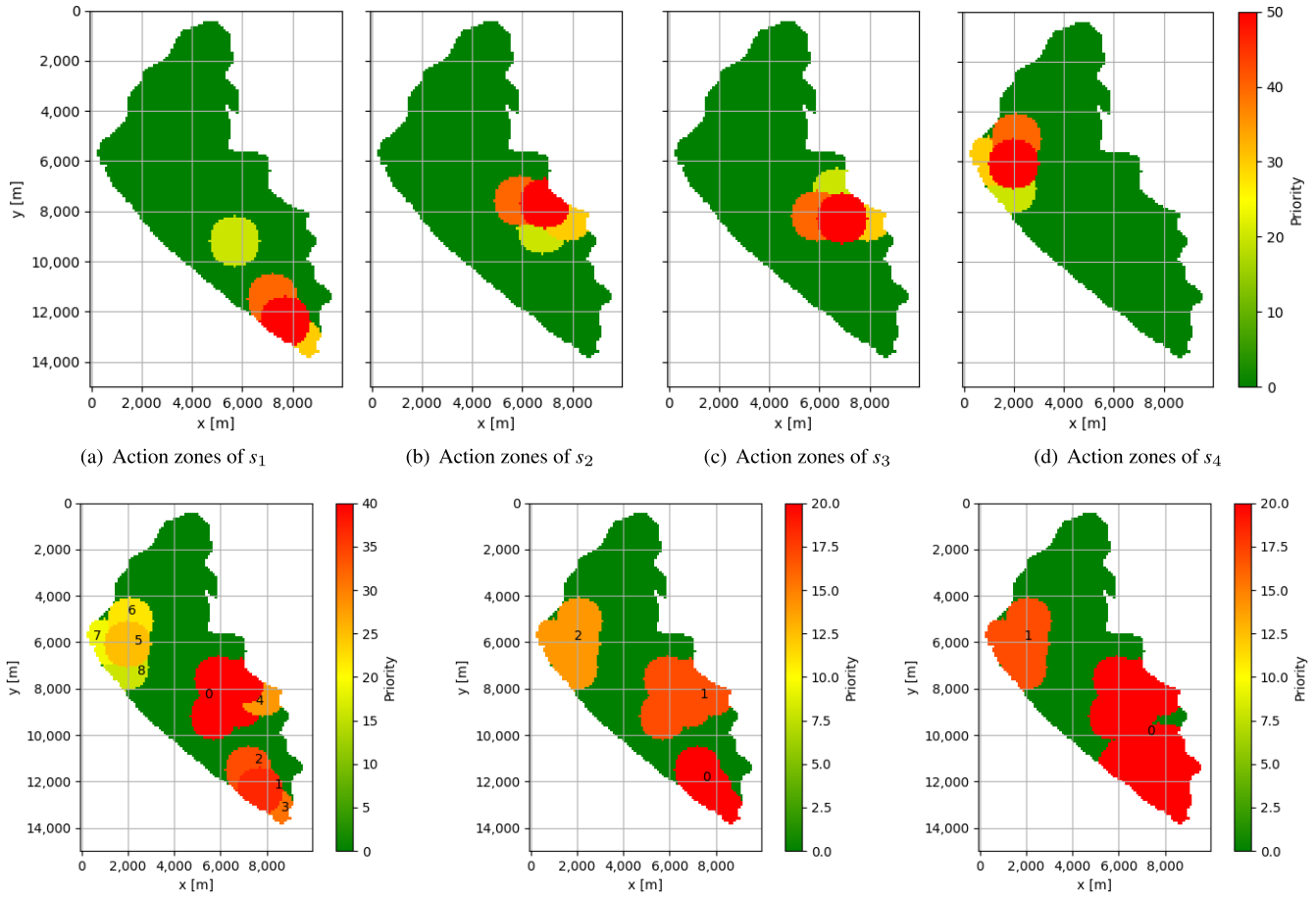

(a) Action zones of s_1 (b) Action zones of s_2 (c) Action zones of s_3 (d) Action zones of s_4

(e) Combined action zones generated in Step 1 (f) Combined action zones generated in Step 2 (g) Combined action zones generated in Step 3

FIGURE 5. Example of the process of generating combined action zones.

TABLE 4. Example of resource allocation: 1st scan.

z	Priority	Number of possibilities	Vehicles
1	1	2	p_1, p_2
2	3	1	p_1
3	1	2	p_2, p_3

TABLE 5. Example of resource allocation: 2nd scan.

z	Priority	Number of possibilities	Vehicles
1	1	1	p_2
3	1	2	p_2, p_3

An example is shown below: considering a fleet with three ASVs ($|\mathcal{P}| = 3$) and three CAZs ($|\mathcal{Z}| = 3$), with the following sensor capabilities for each ASV: $\mathcal{S}_{(p1)} = \{s_1, s_2, s_3\}$, $\mathcal{S}_{(p2)} = \{s_1, s_3, s_4\}$, $\mathcal{S}_{(p3)} = \{s_4\}$; and each CAZ corresponds to the following sensors: $\mathcal{S}_{(z1)} = \{s_1\}$, $\mathcal{S}_{(z2)} = \{s_1, s_2, s_3\}$, $\mathcal{S}_{(z3)} = \{s_4\}$. After the initial scan, the following data is obtained:

Based on this information, it is observed that p_1 has the highest priority since it has the most matches with z_2. Then, $\mathcal{P}_{(z2)} = \{p_1\}$. Following this assignment, a subsequent scan is performed to determine the next optimal assignment based on the remaining vehicles and CAZ:

After the scan, it is observed that both z have the same *Priority*. Therefore, the *Number of possibilities* is taken into consideration. Since z_1 has the lowest value, it is given the highest priority. Then, $\mathcal{P}_{(z1)} = \{p_2\}$. Finally, $\mathcal{P}_{(z3)} = \{p_3\}$.

Algorithm 2 shows the process of the resource allocation phase. In the this phase, action zones are first created for each water quality parameter s. Once all the zones are obtained $\mathcal{A}$, the next step is to generate CAZs $\mathcal{Z}$ and assign vehicles to them $\mathcal{P}_{(z)}$. These two processes are intertwined. If there are any CAZs without assigned vehicles, new CAZs are generated according to the three cases mentioned earlier until all zones have vehicles assigned (*vehicles_assigned*).

c: EXPLOITATION PHASE

After assigning the vehicles to the CAZs, the algorithm proceeds with the exploitation of the areas. Due to the change of target between phases, the speed equation varies. In the

Algorithm 2 AquaHet-PSO Resource Allocation phase Pseudo-Code

```
for sinS do
    A_(s) ← Obtain action zones for each of the WQP
while not vehicles_assigned do
    Z ← Generate combined action zones
    P_(z) ← Assign vehicles to the combined action zones
```

exploitation phase, the speed is calculated according to the results obtained in [38], where the analysis shows that the maximum uncertainty term **max_un** must be eliminated, Eq. 13. To calculate the position, the Classic PSO equation is used, Eq. 4b. Before applying the velocity equation, the Enhanced GP-based PSO components must be calculated using the equations of Section IV-D1.

$$\mathbf{v}_p^{t+1} = w\mathbf{v}_p^t + c_1 r_1^t[\mathbf{pbest}_p^t - \mathbf{x}_p^t] + c_2 r_2^t[\mathbf{gbest}^t - \mathbf{x}_p^t] + c_4 r_4^t[\mathbf{max\_con}^t - \mathbf{x}_p^t] \quad (13)$$

During the exploitation task, measurements are made through sensors available on the ASVs of the fleet. However, not all water quality sensors on the ASVs are used to update their movement. Sensors that do not correspond to the parameters of the CAZs are deactivated, which means that their weight w_{s_p} is set to zero. This is done to prevent parameters not related to the parameters of the CAZs from influencing the exploitation of those regions.

The AquaHet-PSO incorporates the distributed learning technique during the exploitation phase. This system is employed to update the WQPs models within each CAZ. Nevertheless, centralized communication with the central server is maintained and updates are performed at the central server. In the AquaHet-PSO, the CAZs are treated as nodes, which form sub-fleets. Once the vehicles are assigned and the sub-fleets and nodes are established, the corresponding parameter models for each CAZ generated during the exploitation phase are provided. The new measurements obtained during the exploitation phase are combined with the measurements collected during the exploration phase to generate the parameter models. It is important to note that the measurements of the different zones are not mixed. This is applied in order not to influence the calculation of the new positions. The exploitation phase, as well as the monitoring mission, ends when the vehicles have traveled a distance equal to *exploitation_distance*.

From this point on wards, the operation of the algorithm follows a similar pattern to the exploration phase, this can be observed in Algorithm 3. After assigning vehicles to their respective zones, the algorithm continues until the vehicles have traveled a distance equal to *exploitation_distance*. This distance represents the remaining percentage of distance the vehicles can travel during the monitoring mission. The following steps are performed: calculation of the local best $\mathbf{pbest}_p^t$ and global best $\mathbf{gbest}_p^t$ values of each vehicle using Eq. 8a, 8b or Eq. 9a, 9b, depending on the selected method; when the vehicles reach a distance l between measurements, a new measurement is taken for each vehicle, and the GPs of the WQPs are updated, this update is done separately for each CAZ, as each zone is considered independent; calculation of maximum contamination $\mathbf{max\_con}_p^t$ and maximum uncertainty $\mathbf{max\_un}_p^t$; and update of the speed and position of the ASVs. These steps are repeated until the vehicles reach the maximum mission distance *max_dist*, ensuring continuous monitoring and updating of the WQP models (*max_dist* = *exploration_distance* + *exploitation_distance*).

Algorithm 3 AquaHet-PSO Exploitation Phase pseudo-Code

```
while dist ≤ exploitation_distance do
    for pinP do
        pbest_p^t, gbest_p^t ← Obtain the values from Eq. 8 or Eq. 9*;
    dist ← x^t − x_measure ← Calculate distance
    if dist ≥ l then
        for zinZ do
            for pinP_(z) do
                for sinS_(p) do
                    y_s(x) ← Take water resource measurements from the s parameter sensor
            for sinS_(z) do
                σ_{s_z}^t, μ_{s_z}^t ← Adjust the GP of the s parameter
            for pinP do
                max_un_p^t, max_con_p^t ← Obtain the values from Eq. 8 or Eq. 9*
        for pinP do
            v_p^{t+1}, x_p^{t+1} ← Update speed and position of the ASVs using Eq. 13 and Eq. 20b
```

*The terms $\mathbf{pbest}_p$, $\mathbf{gbest}_p$, $\mathbf{max\_un}_p$ and $\mathbf{max\_con}_p$ are calculated according to the selected method, coupled or decoupled.

d: FINAL MODEL

To obtain the final model of the WQPs, the monitoring system combines the measurements collected during the exploration and exploitation phases. All measurements obtained throughout the monitoring process are merged in a central server, which allows updating the corresponding GP associated with each WQP.

3) MEASUREMENTS OF WQPS

Water resource measurements are taken every l distance traveled. The formula used for the calculation of the distance l is shown in Eq. 14. This value is calculated by taking the

length scale radius λ, which is a constant, and the posterior length scale value ℓ^t of the GP [24]. This is due to the processing time of the GP, the more measurements are taken, the longer it takes to adjust the GP.

$$l = \lambda \times \ell^t \tag{14}$$

V. PERFORMANCE EVALUATION

A. SIMULATION SETTINGS

The code was implemented in Python 3.8 using the Scikit-learn, DEAP, and Bayesian Optimization libraries. The Scikit-learn library[1] provides machine learning tools, while DEAP[2] is used for evolutionary algorithm implementation, and Bayesian Optimization library[3] is used for optimizing hyperparameters. The code can be found on GitHub.[4] The simulations were conducted on a laptop computer with an Intel i5 1.60 GHz processor and 8GB RAM.

B. GROUND TRUTH: YPACARAI LAKE

The case of study for testing the monitoring system is the Ypacarai lake. The search space is scaled, each pixel on the map represents an area of 100 × 100 meters, resulting in a search map with dimensions of 100 × 150 meters. The distribution map of the WQPs, also known as ground truth, is generated using the Shekel function, Eq. 15. The Shekel function is a commonly used benchmark function in optimization and modeling tasks, which is multimodal, multidimensional, continuous, and deterministic [24].

$$f_{\text{Shekel}}(\mathbf{x}) = \sum_{i=1}^{M} \frac{1}{c_i + \sum_{j=1}^{L}(x_j - a_{ij})^2} \tag{15}$$

The Shekel function has the advantage of being a multimodal function, which means that it allows for multiple maximum points to exist in the entire search space. These maximum points represents areas in the Ypacarai lake with high levels of contamination of WQPs. Nevertheless, it should be pointed out that in the tests conducted, the correlation between WQPs is not considered. In Eq. 15, the parameters a_{ij} and c_i represent the positions at which the maximum point and the inverse of the significance value of the maximum of the function are located, respectively. The matrix A, to which the element a_{ij} belongs, has dimensions of $M \times L$, where M represents the number of maximum points and L represents the dimension of the space. On the other hand, the matrix C, to which element c_i belongs, has dimensions of $M \times 1$. In the case of the informative path planner tests, the distribution of the maps is generated using the Shekel function. This function generates 50 different sets of S maps, where S represents the number of type of sensors. Each map in the set will have 2 peaks in the (x, y) dimensions, as indicated by the value of 2 for the M and L terms. The positions of the peaks and the values of the matrix C are randomly obtained. An example of a ground truth set generated for a simile is shown in Fig. 6. A different ground truth is generated per WQP sensor.

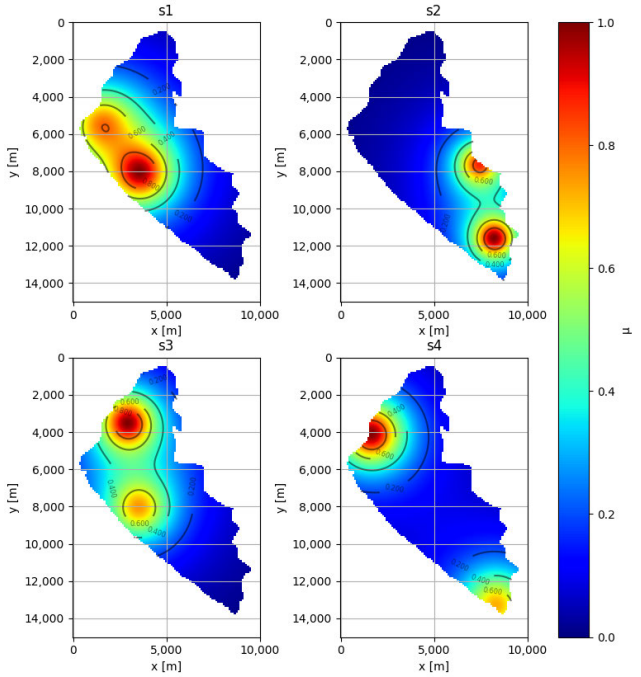

FIGURE 6. Examples of ground truth of water quality parameters obtained with the Shekel function.

Considering that the values of c_i are randomly generated, the data of the generated models are normalized to a range of [0, 1] using Eq. 16:

$$f_{\text{Normalized}}(\mathbf{x}) = \frac{f_{\text{Shekel}}(\mathbf{x}) - f_{\text{min\_Shekel}}(\mathbf{x})}{f_{\text{max\_Shekel}}(\mathbf{x}) - f_{\text{min\_Shekel}}(\mathbf{x})} \tag{16}$$

The normalization process involves utilizing the data obtained from the Shekel function, where $f_{Shekel}(\mathbf{x})$ represents the data, $f_{min\_Shekel}(\mathbf{x})$ represents the minimum value within that data, and $f_{max\_Shekel}(\mathbf{x})$ represents the maximum value obtained.

C. PARAMETER SETTINGS

The simulation experiments involve fleets of 5 to 10 vehicles, with the number of vehicles being chosen randomly. Each test consists of 50 simulations. The number of sensors of the same type varies from one method or informative path planner to another, ranging from 2 to 6 sensors. This enables the observation of the behavior of the methods or informative path planners with different numbers of ASVs that can measure the same WQP. Additionally, a test is conducted where the number of sensors of the same type is variable, ranging from 4 to 6 sensors. Each ASV can have up to three sensors measuring different WQPs on board. To determine the value of λ in Eq. 14, the studies performed in [14] and [24] are considered. In order to reduce the computational time and

[1] https://scikit-learn.org/stable/index.html (accessed on 22 June 2023).
[2] https://deap.readthedocs.io/en/master/ (accessed on 22 June 2023).
[3] https://github.com/fmfn/BayesianOptimization (accessed on 22 June 2023).
[4] https://github.com/MicaelaTenKathen/AquaHet-PSO.git (accessed on 22 June 2023).

to obtain enough measurements to generate good models of the WQPs, the value of λ is set at 0.3. According to [39], in order for the GP to generate smooth models, the length scale value must be 10% of the search space length value. Based on this information, the length scale of the GPs are uniformly set to 10, since the map is scaled.

To determine the weights of each WQP function (w_{s_p}), in the coupled method, the number of sensors in the fleet of ASVs is taken into account, the more sensors of the same parameter, the lower the weight value of that parameter. This is applied in order to give more priority to the sensors that are less available. To obtain the values, Eq. 11 is applied at the beginning of each simulation. It is important to mention that the weights of the sensors s differ from one ASV p to another, as they depend on the sensors installed on each ASV.

For the weights of the terms of Eq. 12 and Eq. 13, c_1, c_2, c_3, c_4, in the exploration phase, the values obtained in [37] are used, and for the exploitation phase, the weights are set to the values obtained in [38]. The studies mentioned earlier were specifically conducted for a fleet of 4 vehicles, which in the case of the AquaHet-PSO, refers to 4 sensors of the same type. Therefore, for a different number of vehicles, the weight values used in the algorithm vary. The weight values for these scenarios can be found in Table 9 of the Appendix B. The values of the weights of c shown in Table 6 are for a number of 4 sensors or more. In the AquaHet-PSO, first, the ASVs travel 10km to obtain data from the entire surface of the lake, focusing on the exploration of the water resource. After collecting the necessary data, the ASVs focus on characterizing the areas where the highest levels of contamination are found. During the exploitation phase, each ASV covers a distance of 10km. These values were determined according to the study performed in [25]. This study demonstrated that a balanced ratio of 50% exploration distance (*exploration_distance*) and 50% exploitation distance (*exploitation_distance*) is optimal. As a result, the maximum distance *max_dist* for the monitoring mission is set at 20km. To determine the radius of the action zones *rad*, the value set in the length scale is taken into account. The goal is to ensure that there are no significant changes between the positions of the measurements within the zones. All parameters and hyper-parameters that are set are shown in Table 6.

TABLE 6. Parameter values for informative path planner tests.

Component	Parameter	Value
Simulation parameters	Number of vehicles ($\|\mathcal{P}\|$)	5 - 10 vehicles
	Type of WQP sensors	2 - 10 WQPs
	Number of sensors of the same type	2 - 6 sensors
	Simulations	50 simulations
	max_dist	20km
Gaussian process	ℓ_0	10
	$\ell bounds$	$[1 \times 10^{-5}, 10]$
AquaHet-PSO	λ	0.3
	$c_{1explore}$	2.0187
	$c_{2explore}$	0
	$c_{3explore}$	3.2697
	$c_{4explore}$	0
	$c_{1exploit}$	3.6845
	$c_{2exploit}$	1.5614
	$c_{3exploit}$	0
	$c_{4exploit}$	3.1262
	exploration_distance	10km
	exploitation_distance	10km
	rad	1km (10)
Genetic algorithm	individual	list of indices size $\|\mathcal{P}\|$
	population	$10*\|\mathcal{P}\|$
	generations	$10*\|\mathcal{P}\|$
	crossover probability	0.5
	crossover function	Ordered
	mutation probability	0.5
	mutation function	Shuffle Indices
	Algorithm	EA $\mu + \lambda$
	Selection function	Tournament (size=3)
	fitness	max sensor distance (Eq. 7)

D. PERFORMANCE METRICS

The main objective of the proposed monitoring system is to minimize the discrepancy between the actual models of the water quality parameters $y_s(x_i)$ and their estimated models $\hat{y}_s(x_i)$, as discussed in Section III-A. In addition to using Mean Squared Error (MSE) across the entire search space, Eq. 2, as a comparison metric, the following metrics are also utilized:

1) **R-squared (R^2):** It measures the goodness of fit between the ground truths $y_s(x_i)$ and the estimated models $\hat{y}_s(x_i)$ across the entire search space $\mathcal{N}$. The term N represents the number of elements of the set $\mathcal{N}$, S represents the number of elements of the set $\mathcal{S}$, and the term $\bar{y}_s(x)$ is the average of the values. To obtain the R^2 value of the monitoring system, Eq. 17 is applied. It is first necessary to calculate the R^2 between each ground truth and estimated model of the sensors that compose the set $\mathcal{S}$. Then, the average of the results is obtained.

$$R^2{}_{map}(y_s, \hat{y}_s) = \frac{1}{S}\sum_{s=1}^{S}\left(1 - \frac{\sum_{i=1}^{N}(y_s(x_i) - \hat{y}_s(x_i))^2}{\sum_{i=1}^{N}(y_s(x_i) - \bar{y}_s(x))^2}\right) \quad (17)$$

2) **Peak Error:** It calculates the difference between the peaks of the CAZs in the ground truth $y_s(x_i)$ and estimated models $\hat{y}_s(x_i)$ by applying Eq. 18. This metric provides insight into the error associated with the detection of contamination peaks. The term Z_{peaks} represents the number of contamination peaks detected using the CAZ. The error is calculated by taking the average of the errors of the peaks in the CAZ associated with the CAZ sensors ($\mathcal{S}_z$). Subsequently, the average of these CAZ errors is computed. The term S_z refers to the number of WQPs belonging to CAZ.

$$\text{Error}_{peak}(y_s, \hat{y}_s) = \frac{1}{Z_{peaks}}\sum_{z=1}^{Z} \times \left(\frac{1}{S_z}\sum_{s=1}^{S_z}(|y_s(x_i) - \hat{y}_s(x_i)|)\right) \quad (18)$$

3) **MSE of CAZs:** It calculates the average squared difference between the ground truth $y_s(x_i)$ and estimated models $\hat{y}_s(x_i)$ specifically for the CAZs. This value is obtained using Eq. 19. To calculate the MSE in the CAZs, first, the MSE between the ground truth and the estimated models of the sensors that form the CAZ ($\mathcal{S}_{\ddagger}$), is computed. Then, the average of these MSE results is calculated, considering the CAZs. It is important to note that the MSE is calculate specifically for the areas (coordinates) that compose the CAZs. The Z_{coord} corresponds to the number of coordinates that constitute the CAZs.

$$\mathrm{MSE}_{CAZ}(y_s, \hat{y}_s) = \frac{1}{Z_{coord}} \sum_{z=1}^{Z} \times \left(\frac{1}{S_z} \sum_{s=1}^{S_z} (y_s(x_i) - \hat{y}_s(x_i))^2 \right) \quad (19)$$

E. DECOUPLED METHOD VS COUPLED METHOD

This subsection presents a comparison between the AquaHet-PSO variants, the decoupled and the coupled methods. In the decoupled method, the monitoring system prioritizes only one vehicle sensor during each time period, whereas in the coupled method, all ASV sensors influence the movement of the vehicles, giving priority to the WQP with the fewest sensors in the fleet.

Apart from comparing the methods, the impact of the initial positions of the ASVs is also assessed. The study analyzes the behaviors of the methods when the GA is applied to assign the starting points of the vehicles, as well as when the distribution of the vehicles is not maximized (without GA). An example of this application is shown in Fig. 4, where the initial positions of the vehicles are shown without using the GA (Fig. 4(a)), and Fig. 4(b) shows the new initial positions by applying the maximization of the initial distance between the ASVs (GA). These tests are conducted considering different numbers of sensors of the same type. The results are shown in Table 7.

Fig. 7 shows the results obtained for the case of 4 or more sensors in boxplot format, where AquaHet-PSO-C-GA is the abbreviation for the coupled method of the AquaHet-PSO using the GA for the initial positioning of the ASVs, the AquaHet-PSO-C for the coupled method of AquaHet-PSO without the use of the GA, AquaHet-PSO-D-GA refers to the decoupled method of AquaHet-PSO using the GA for the initial GA positions and AquaHet-PSO-D refers to the decoupled method of AquaHet-PSO without using the GA.

The test results show that the coupled method, which uses the GA to assign the initial positions of the ASVs, performs better than the other methods. This can be attributed to the fact that all sensors influence the motion of the vehicles, i.e., the optimal positions of each sensor are considered to determine the next position.

In contrast, the decoupled method, where only one sensor is prioritized per time period, has limitations. Vehicles are unable to effectively scan optimal zones for other sensors, resulting in deficient model generation where the pollution zones for those sensors do not approach the actual pollution zones. Consequently, the exploitation of high pollution zones and the detection of pollution peaks related to non-priority sensors is adversely affected.

In summary, the decoupled method may present some poor results in both exploration and exploration. Constantly changing priority with respect to sensors can result in overlapping paths in the exploration phase limiting exploration of unexplored areas. Additionally, in the exploitation phase, focusing on a single sensor results in poor exploitation of the other WQPs. Based on these results, the AquaHet-PSO coupled method is selected to compare with the other informative path planners.

The performance of the coupled AquaHet-PSO method, with GA for initial ASV positioning, is evaluated for several numbers of sensors of the same type of WQP. Fig. 8 shows the results obtained as a function of the average distance traveled by the fleet vehicles. In each test, the fleets consist of the same number of identical-sensors, except for the scenario with 4 or more sensors, where the fleets can have between 4 or 6 sensors of the same type. The results indicate that the proposed monitoring system performs well when there are 4 or more sensors of the same type. This is because with a small number of sensors of the same type, the system struggles to generate an accurate initial model during the exploration phase, leading to limited creation of CAZs in areas with higher contamination levels. Consequently, the detection of contamination peaks becomes challenging. Therefore, having a limited number of sensors of the same type and that vehicles may possess multiple sensors, the swarm is unable to effectively detect local optima or contamination zones throughout the search space. Nevertheless, when an ASV is equipped with multiple sensors, its focus is distributed among different parameters, potentially impacting the exploration and exploitation of each parameter.

F. COMPARISON OF MULTI-OBJECTIVE AND HETEROGENEOUS INFORMATIVE PATH PLANNERS

In this subsection, the performance of multi-objective and heterogeneous path planners is compared. The parameters of all path planners are set with the same values shown in Table 6, including the number of vehicles (N), number of sensors (S), length scale of GPs, among others.

One of the informative path planners that is compared is the lawnmower algorithm. The implementation of this algorithm is based on the code provided by [40]. The interspace parameter is set to match the Gaussian Process (GP) length scale, which is 10. This ensures that there are minimal variations between sensor measurements taken at different positions. The initial positions of the ASVs in the lawnmower

TABLE 7. Comparison of AquaHet-PSO variants.

Sensors of the same type	Method		R2 Score	MSE Map	Error (Peaks)	MSE (CAZ)
2 sensors	Decoupled	With GA	0.4022 ± 0.4148	0.0255 ± 0.0186	0.3283 ± 0.1509	0.0833 ± 0.0715
		Without GA	0.1833 ± 0.6168	0.0349 ± 0.0259	0.3957 ± 0.2133	0.1170 ± 0.0987
	Coupled	**With GA**	**0.4852 ± 0.4292**	**0.0219 ± 0.0189**	**0.3147 ± 0.1170**	**0.0719 ± 0.0740**
		Without GA	0.3334 ± 0.4948	0.0281 ± 0.0207	0.3484 ± 0.1834	0.0914 ± 0.0727
3 sensors	Decoupled	With GA	0.6909 ± 0.3012	0.0129 ± 0.0125	0.2657 ± 0.1741	0.0419 ± 0.0504
		Without GA	0.4574 ± 0.4813	0.0230 ± 0.0197	0.3304 ± 0.2160	0.0752 ± 0.0770
	Coupled	**With GA**	**0.7520 ± 0.2764**	**0.0103 ± 0.0119**	**0.2190 ± 0.1783**	**0.0328 ± 0.0465**
		Without GA	0.5724 ± 0.4847	0.0183 ± 0.0204	0.2878 ± 0.2198	0.0605 ± 0.0817
4 sensors	Decoupled	With GA	0.9128 ± 0.1207	0.0039 ± 0.0057	0.1790 ± 0.1629	0.0131 ± 0.0221
		Without GA	0.7957 ± 0.3459	0.0089 ± 0.0153	0.2239 ± 0.2292	0.0288 ± 0.0543
	Coupled	**With GA**	**0.9499 ± 0.0850**	**0.0022 ± 0.0041**	**0.1576 ± 0.1546**	**0.0069 ± 0.0158**
		Without GA	0.8806 ± 0.2055	0.0049 ± 0.0081	0.1871 ± 0.1810	0.0160 ± 0.0326
5 sensors	Decoupled	With GA	0.9640 ± 0.0646	0.0013 ± 0.0019	0.1483 ± 0.1638	0.0047 ± 0.0094
		Without GA	0.8856 ± 0.2326	0.0049 ± 0.0095	0.1938 ± 0.1751	0.0164 ± 0.0359
	Coupled	**With GA**	**0.9692 ± 0.0741**	**0.0012 ± 0.0024**	**0.1447 ± 0.1642**	**0.0040 ± 0.0121**
		Without GA	0.9467 ± 0.1450	0.0025 ± 0.0072	0.1620 ± 0.1531	0.0079 ± 0.0263
6 sensors	Decoupled	With GA	0.9747 ± 0.0506	0.0010 ± 0.0018	0.1525 ± 0.1632	0.0035 ± 0.0080
		Without GA	0.9591 ± 0.0996	0.0017 ± 0.0043	0.1588 ± 0.1803	0.0058 ± 0.0175
	Coupled	**With GA**	**0.9809 ± 0.0782**	**0.0007 ± 0.0029**	**0.1434 ± 0.1845**	**0.0027 ± 0.0141**
		Without GA	0.9641 ± 0.1146	0.0016 ± 0.0058	0.1495 ± 0.1679	0.0057 ± 0.0245
4 or more sensors	Decoupled	With GA	0.9387 ± 0.0992	0.0028 ± 0.0049	0.1777 ± 0.1617	0.0096 ± 0.0216
		Without GA	0.8392 ± 0.2664	0.0069 ± 0.0109	0.2141 ± 0.1823	0.0242 ± 0.0446
	Coupled	**With GA**	**0.9577 ± 0.0898**	**0.0018 ± 0.0044**	**0.1541 ± 0.1705**	**0.0060 ± 0.0188**
		Without GA	0.9180 ± 0.1794	0.0033 ± 0.0067	0.1757 ± 0.1672	0.0111 ± 0.0294

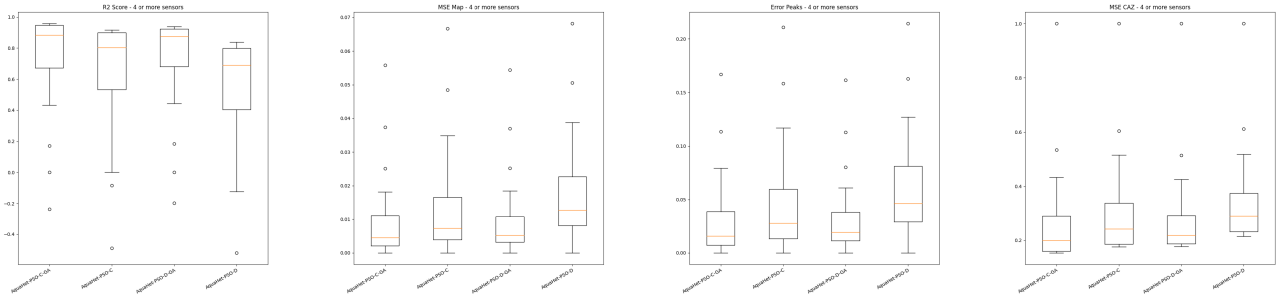

(a) Results of the R^2 of the whole water resource models. (b) Results of the MSE of the whole water resource models. (c) Results of the peak errors. (d) Results of the MSE of the combined action zone models.

FIGURE 7. Distribution of the obtained results for the AquaHet-PSO methods using the GA and without using the GA for the initial positioning of the ASVs.

algorithm are the same as those used in the AquaHet-PSO method without GA.

Table 8 presents the results obtained from the tests performed for different numbers of sensors of the same type. It can be seen that for a low number of sensors of the same type, the lawnmower outperforms the coupled AquaHet-PSO method. As mentioned above, having a low number of sensors of the same type and the possibility of each ASV having more than one sensor on board makes it difficult to explore the surface of the water resource. This is because the vehicle needs to cover a larger area of the water resource and to explore the surface it must consider the best local and uncertainty of all the sensors on board. Consequently, it also affects the segmentation of the lake and the detection of contamination peaks. As the number of sensors of the same WQP increases, the monitoring system can cover a larger area of the water resource, allowing more measurements and improving the initial model. This facilitates the creation of CAZs in regions with higher pollution potential, resulting in better detection of pollution peaks. Starting with a minimum of four sensors of the same type, the AquaHet-PSO shows a significant performance improvement compared to lawnmower. These results can be seen in the form of a boxplot in Fig. 9. Additionally, the results during the mission, in terms of the average distance traveled by the ASVs, are shown visually in Fig. 10. Fig. 10 shows the results obtained with respect to the lawnmower and AquaHet-PSO methods for the case of 4 or more sensors during the monitoring mission. Initially, the lawnmower method outperforms the AquaHet-PSO in the tests. However, as the mission progresses, the AquaHet-PSO demonstrates better performance. This difference in performance can be attributed to several factors. With the lawnmower method, the ASVs thoroughly explore the surface at the beginning of the mission. However, this method does not account for model uncertainty and does not effectively exploit areas of increased contamination. As a result, the lawnmower method may not generate the most accurate models of WQPs

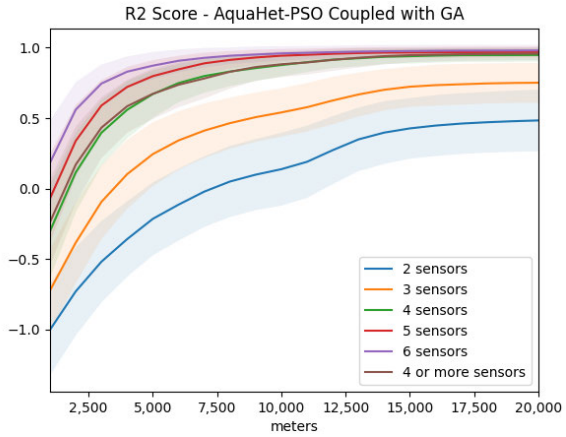

(a) Mean and standard deviation of the R^2 of the whole water resource models.

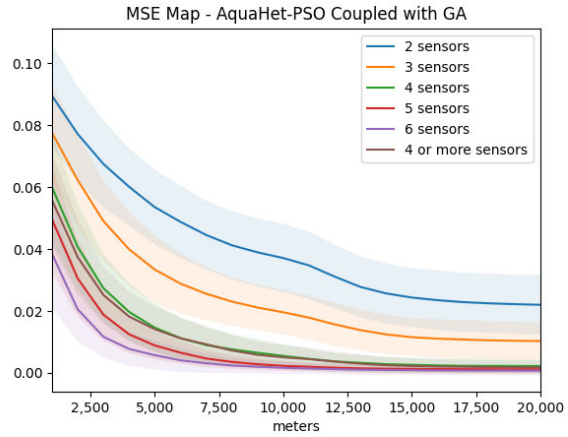

(b) Mean and standard deviation of the MSE of the whole water resource models.

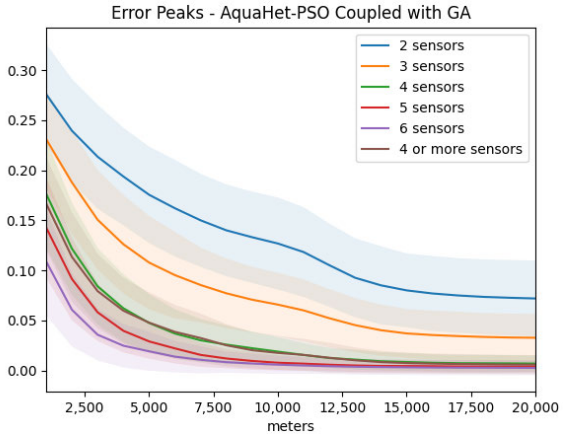

(c) Mean and standard deviation of the peak errors.

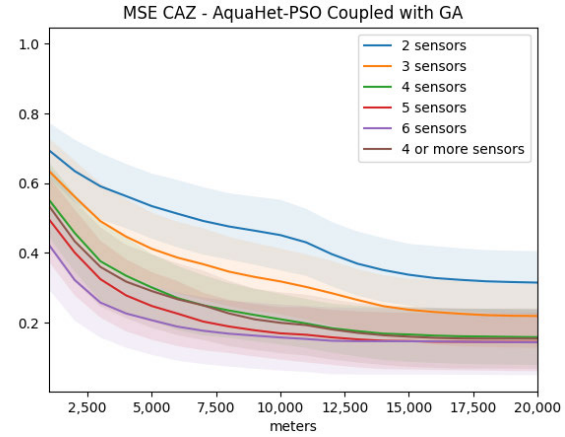

(d) Mean and standard deviation of the MSE of the combined action zone models.

FIGURE 8. Results obtained using the coupled AquaHet-PSO method, which incorporates the use of GA for assigning the starting points of ASVs, for various numbers of sensors of the same type.

TABLE 8. Performance comparison of informative path planners for different numbers of sensors of the same type.

Sensors of the same type	Informative Path Planner		R2 Score	MSE Map	Error (Peaks)	MSE (CAZ)
2 sensors	**Lawnmower**		**0.5128 ± 0.3945**	**0.0214 ± 0.0179**	**0.2945 ± 0.1766**	**0.0694 ± 0.0847**
	AquaHet-PSO	With GA	0.4852 ± 0.4292	0.0219 ± 0.0189	0.3147 ± 0.1170	0.0719 ± 0.0740
		Without GA	0.3334 ± 0.4948	0.0281 ± 0.0207	0.3484 ± 0.1834	0.0914 ± 0.0727
3 sensors	Lawnmower		0.6427 ± 0.3784	0.0162 ± 0.0173	0.2414 ± 0.1882	0.0469 ± 0.0643
	AquaHet-PSO	**With GA**	**0.7520 ± 0.2764**	**0.0103 ± 0.0119**	**0.2190 ± 0.1783**	**0.0328 ± 0.0465**
		Without GA	0.5724 ± 0.4847	0.0183 ± 0.0204	0.2878 ± 0.2198	0.0605 ± 0.0817
4 sensors	Lawnmower		0.7815 ± 0.2821	0.0089 ± 0.0109	0.1926 ± 0.1755	0.0219 ± 0.0439
	AquaHet-PSO	**With GA**	**0.9499 ± 0.0850**	**0.0022 ± 0.0041**	**0.1576 ± 0.1546**	**0.0069 ± 0.0158**
		Without GA	0.8806 ± 0.2055	0.0049 ± 0.0081	0.1871 ± 0.1810	0.0160 ± 0.0326
5 sensors	Lawnmower		0.8918 ± 0.2245	0.0048 ± 0.0098	0.1544 ± 0.1676	0.0092 ± 0.0286
	AquaHet-PSO	**With GA**	**0.9692 ± 0.0741**	**0.0012 ± 0.0024**	**0.1447 ± 0.1642**	**0.0040 ± 0.0121**
		Without GA	0.9467 ± 0.1450	0.0025 ± 0.0072	0.1620 ± 0.1531	0.0079 ± 0.0263
6 sensors	Lawnmower		0.9182 ± 0.2205	0.0034 ± 0.0092	0.1588 ± 0.1664	0.0061 ± 0.0182
	AquaHet-PSO	**With GA**	**0.9809 ± 0.0782**	**0.0007 ± 0.0029**	**0.1434 ± 0.1845**	**0.0027 ± 0.0141**
		Without GA	0.9641 ± 0.1146	0.0016 ± 0.0058	0.1495 ± 0.1679	0.0057 ± 0.0245
4 or more sensors	Lawnmower		0.7935 ± 0.4354	0.0085 ± 0.0140	0.1920 ± 0.1607	0.0198 ± 0.0450
	AquaHet-PSO	**With GA**	**0.9577 ± 0.0898**	**0.0018 ± 0.0044**	**0.1541 ± 0.1705**	**0.0060 ± 0.0188**
		Without GA	0.9180 ± 0.1794	0.0033 ± 0.0067	0.1757 ± 0.1672	0.0111 ± 0.0294

over time. In contrast, the AquaHet-PSO considers the model uncertainty and actively scans unexplored areas to minimize uncertainty. In addition, during the exploitation phase, ASVs focus on areas with a high risk of contamination and collect more measurements to generate the best possible models. This combination of exploration and exploitation strategies

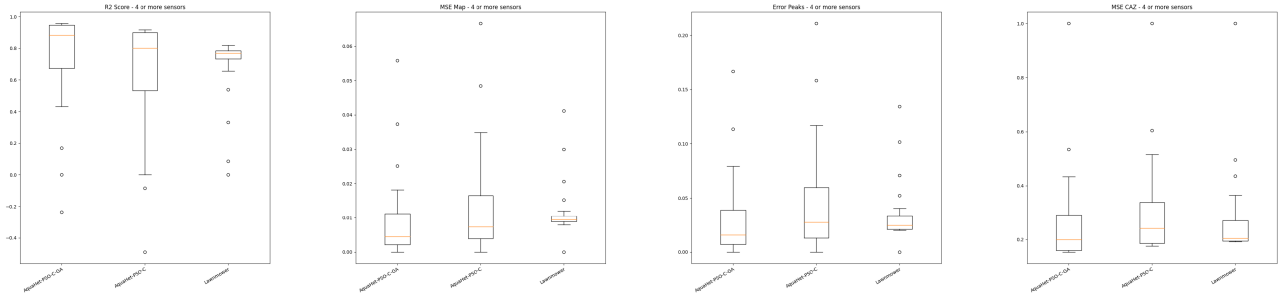

(a) Results of the R^2 of the whole water resource models. (b) Results of the MSE of the whole water resource models. (c) Results of the peak errors. (d) Results of the MSE of the combined action zone models.

FIGURE 9. Distribution of the obtained results from the informative path planners compared in Table 8.

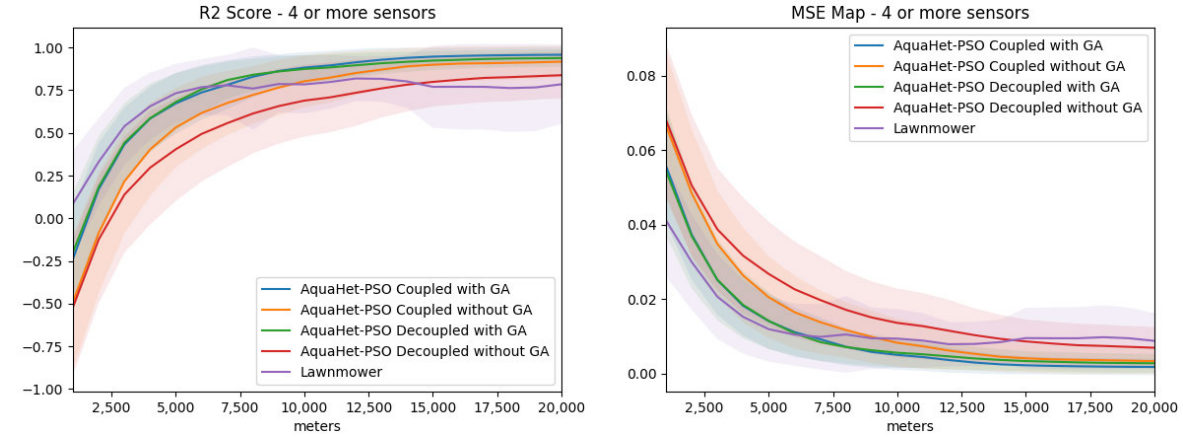

(a) Mean and standard deviation of the R^2 of the models of the entire water resource. (b) Mean and standard deviation of the MSE of the models of the entire water resource.

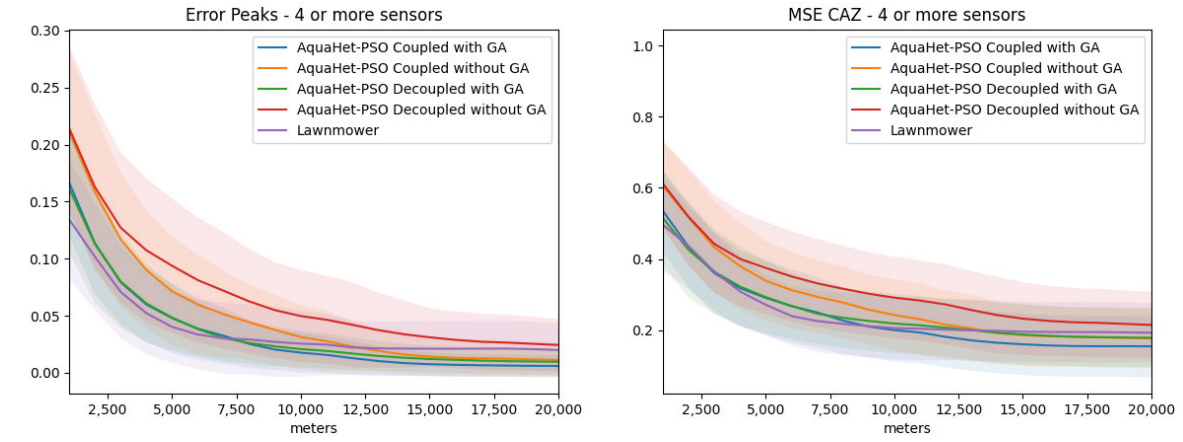

(c) Mean and standard deviation of the peak errors. (d) Mean and standard deviation of the MSE of the models of the combined action zones.

FIGURE 10. Results obtained from the informative path planners during the monitoring task for fleets with 4 or more sensors of the same type.

allows the AquaHet-PSO to outperform the lawnmower method as the mission progresses.

Fig. 11 and Fig. 12 depict monitoring missions conducted using the lawnmower and the AquaHet-PSO monitoring systems, respectively. The missions involve a fleet of 8 vehicles equipped with 4 sensors for each of the 4 WQPs. The ground truth of the WQPs can be seen in Fig. 6, which is located in Section V-B. In Fig. 11, the initial positions of the ASVs are not optimized but randomly selected from either port or clearing points in the Ypacarai lake. Fig. 11(a) illustrates the movement of the ASVs during the mission, while Fig. 11(b) showcases the WQP models obtained at

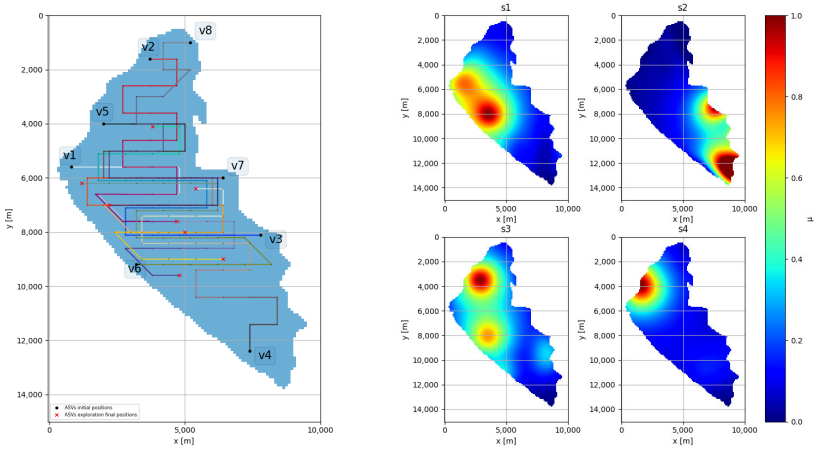

(a) Trajectories performed by the ASVs.

(b) Models of water quality parameters obtained at the end of the monitoring mission.

FIGURE 11. Example of the performance of the Lawnmower. The fleet has the same characteristics as the AquaHet-PSO example (Fig. 8). In the ASV movement graphs, the trajectory of the vehicles is represented in different color.

the conclusion of the mission. Due to the random initial positioning of the ASVs, the lawnmower may not capture all contamination peaks effectively. This discrepancy is evident when comparing the ground truth of parameter s_4 (Fig. 6) with the model generated by the monitoring system (Fig. 11(b)).

On the other hand, the AquaHet-PSO takes advantage of the GA algorithm to optimize the initial positioning of ASVs. This approach ensures a larger coverage of the surface of the Ypacarai lake by maintaining a significant separation between ASVs equipped with the same sensor. The movement and initial positions of ASVs during the exploration phase are depicted in Fig. 12(a). In this figure, the dispersion of vehicle movement is evident as the active terms are the best local and maximum uncertainty, enabling the exploration of uncharted areas. Fig. 12(b) presents the initial models of WQPs obtained at the end of the exploration phase. Comparing these initial models with the final model of the lawnmower method highlights the importance of maximizing the initial positions of ASVs. After covering a distance of 10 km, the proposed system successfully detects potential contamination zones. These zones are delineated through the second phase of AquaHet-PSO. Fig. 12(c) illustrates the operation of the second phase, where 5 CAZs are determined based on the initial models obtained. ASVs are then assigned to their respective zones. When a sufficient number of ASVs is available, the zones are generated according to Step 1 in Section IV-D2b. CAZ 0, being the largest, accommodates three ASVs and focuses on exploiting three WQPs. CAZ 1 has two ASVs assigned to exploit two parameters. Finally, CAZs 2, 3, and 4 correspond to individual parameters, with one ASV assigned to each zone. Fig. 12(d) illustrates the movement of the ASV from the end of the exploration phase to the corresponding CAZs and the movement during the exploitation phase. It is worth noting that while the ASV moves towards its assigned zone, it continues to take measurements. By prioritizing best local, best global, and maximum contamination terms, the ASV movements are concentrated in areas with high contamination levels. In Fig. 12(e), the models generated for each WQP in the respective CAZs are shown. Adding up the parameters measured in each zone results in 8 GPs, leading to the generation of 8 models in the exploitation phase: 3 in CAZ 0, 2 in CAZ 1, and 1 each in CAZs 2, 3, and 4. To obtain the final model for each WQP, the measurements collected by the ASVs are fused in the central server, resulting in a single model for each parameter. Fig. 12(f) demonstrates that the generated models closely resemble the ground truth values of the corresponding parameters.

The computational time needed for an AquaHet-PSO monitoring mission is contingent on the number of samples taken and the quantity of WQPs under monitoring. In other words, as the number of sensors and monitored WQPs increases, the complexity of the mission escalates, resulting in longer computational durations. The duration of a monitoring mission can range from approximately 7 seconds in scenarios involving a fleet of 5 vehicles, each measuring 2 WQPs with 2 sensors for each WQP, to the most intricate case studied, which lasts 53 seconds. This complex scenario involves a fleet of 10 vehicles monitoring 10 WQPs, with each WQP equipped with 2 sensors. These investigations were carried out within the specified constraints, allowing each vehicle to carry up to 3 sensors and considering a maximum of 10 WQPs to monitor (as detailed in Table 6).

G. DISCUSSION OF THE RESULTS

The main results obtained in this work are presented below:

- The coupled and decoupled methods of AquaHet-PSO differ in the information they consider to guide the ASVs. While in the coupled method, information from

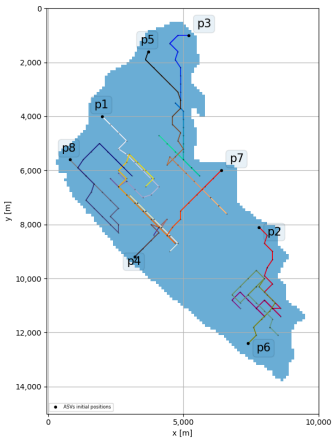

(a) Trajectories performed by the ASVs in the exploration phase.

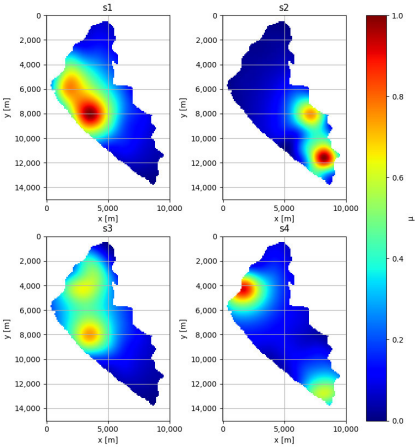

(b) Models of water quality parameters obtained in the exploration phase.

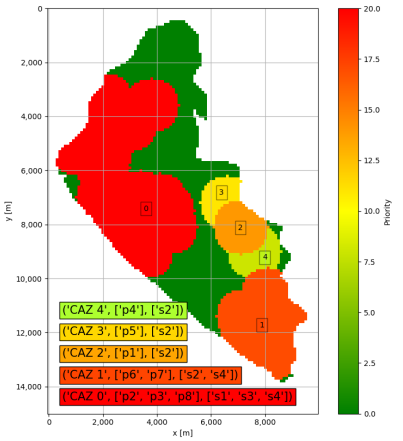

(c) Segmentation of the Ypacarai lake into combined action zones and allocation of ASVs.

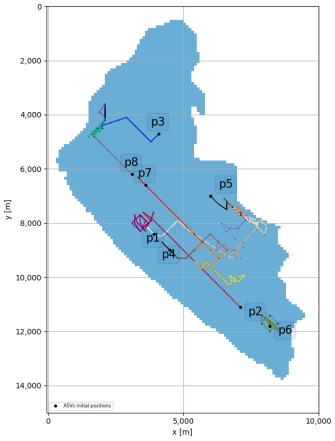

(d) Trajectories performed by the ASVs in the exploitation phase.

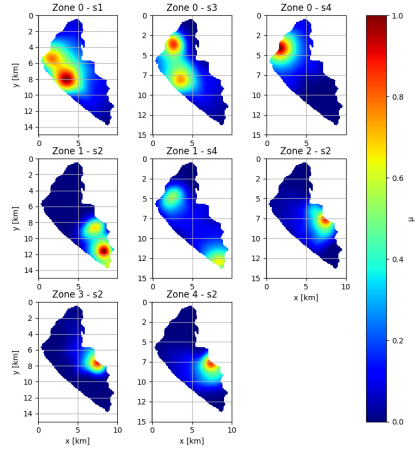

(e) Models of water quality parameters of the combined action zones obtained in the exploitation phase.

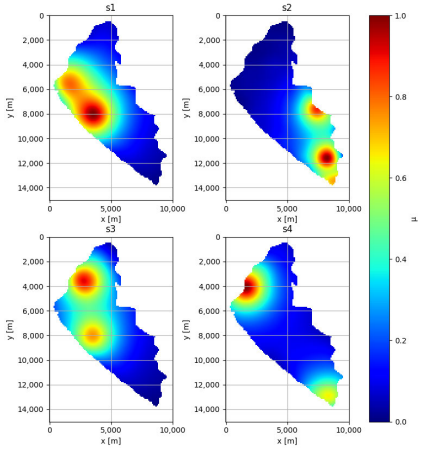

(f) Final models of water quality parameters obtained at the end of the monitoring mission.

FIGURE 12. Example of the performance of the proposed monitoring system. The example shows the 3 phases of the AquaHet-PSO. In the ASV movement graphs, the trajectory of the vehicles is represented in different color.

all sensors in the ASV are considered, in the decoupled method, the algorithm gives priority to information from a single sensor per time period. However, prioritizing only one sensor per time period affects the generation of the models and the detection of the contamination peaks of the other water quality parameters. In the course of the mission, the ASV focuses on exploiting the parameter that has the maximum values of the terms, and it may be the case that such information is always from the same parameter, detracting from the priority of the other parameters.

- The use of the genetic algorithm to select the initial position of the ASVs plays an important role in improving the performance of the AquaHet-PSO. Maximizing the distance between ASVs having the same type of sensor allows to cover a larger area of the water resource in the exploration of the resource. Therefore, potential contamination zones can be detected more effectively.
- When there are few sensors of identical type in the ASV fleet, the lawnmower algorithm proves to be more effective in dealing with heterogeneous and multi-objective problems. However, to navigate the water resource, the AquaHet-PSO uses information from all sensors on board the ASV. As a consequence, the proposed monitoring system may be less advantageous in scenarios where with small number of sensors of the same type because the maximum uncertainty or contamination of the sensors on board the ASV can be at opposite extremes. As a result, the ASV might not detect all possible contamination sources in the exploration phase, which may affect the effectiveness of the other phases of the AquaHet-PSO.
- On the contrary, when the number of identical sensors is higher, the AquaHet-PSO performs better than the lawnmower. Guided by data from more than one water quality parameter is not as advantageous with a

small number of identical sensors. However, when the number is larger, this weakness becomes the strength of the algorithm. It allows measurements to be obtained from different types of sensors in optimal positions. As a consequence, it is possible to detect regions with possible contamination hotspots. With these first approximations, possible action zones are delimited and exploited, resulting in the detection of pollution peaks and the generation of good models of water quality parameters. The results for R^2 of the lawnmower with respect to the coupled method of the AquaHet-PSO with GA decrease by 17% in the case of 4 or more sensors. In addition, there is an improvement of approximately 370% in the generation of water quality parameter models over the entire search space, a 24% improvement in the detection of contamination peaks and a 230% improvement in the characterization of water quality parameters in areas of potential contamination.

VI. CONCLUSION AND FUTURE WORK

A multi-objective monitoring system for a fleet of heterogeneous ASVs has been developed and simulated in this work, the AquaHet-PSO. The proposed monitoring system is based on the PSO, the GP, and the GA. It makes use of the GP as a surrogate model. The GP allows the generation of complete models for water quality parameters, which facilitates the estimation of data on the entire water resource. The objectives of the AquaHet-PSO are to generate good models of multiple quality parameters itself, and to detect pollution peaks of these parameters. The ASV fleet is composed of vehicles that do not have the same water quality parameter measurement capabilities, which we call heterogeneous ASV fleet. By applying the GA, the initial positions of ASVs with identical sensors can be optimized, allowing increased coverage of a wider area from the beginning of the monitoring mission. Then, the operation of the AquaHet-PSO consists of three phases. The first phase is the exploration phase. In this first phase, the aim is to cover the largest possible area of water resource in order to generate good first models of water quality parameters. The first models generated are used in the second phase of the algorithm. In the second phase, called resource allocation, the regions where potential areas with high contamination levels are detected (combined action zones) are delimited and ASVs are assigned to these regions. The ASVs are assigned according to the sensors they possess and the water quality parameters measured in each zone. This phase aims to optimize measurements and focus on areas with high pollution levels by taking advantage of the capability of ASVs to have on board several different sensors. This approach allows the collection of data for different water quality parameters within the combined action zones, which improves measurement efficiency and zone characterization. Finally, the exploitation phase. In this phase, the ASVs focus on characterizing the water quality parameters in depth, taking measurements in the combined action zones. The distributed learning technique is used in the exploitation phase so that each sub-fleet assigned to the action zones operates independently of the other fleets. This allows the ASVs to focus only on the zone to which they are assigned. The generation of the final models is performed on the central server at the end of the three phases mentioned above. The measurements of the combined action zones are merged to obtain the final models of the water quality parameters. The results of the study showed the effectiveness of the monitoring system in meeting the challenges related to multi-objective monitoring missions and heterogeneous fleets. In addition, the importance of strategic initial vehicle positioning for simultaneous monitoring of multiple water quality parameters was validated. The AquaHet-PSO successfully generated accurate models for water quality parameters, performed comprehensive characterization of potentially contaminated areas, and detected pollution peaks for each parameter. As future work, the monitoring system will be improved by integrating the Pareto dominance method instead of the scalarization of the objectives to calculate the PSO components and the coordinates of maximum contamination and uncertainty. Furthermore, it is proposed to implement the monitoring system in a real-world heterogeneous fleet of ASVs for further validation and evaluation. Additionally, research will be conducted to develop informative path planning solutions for heterogeneous fleets based on alternative heuristic algorithms.

APPENDIX A
ENHANCED GP-BASED PSO

The Enhanced GP-based PSO is a monitoring system that is based on the PSO and has the GP as surrogate model [14]. In the Enhanced GP-based PSO, the number of sensors S is considered equal to 1, i.e., only the modeling of a WQP is considered. Since it is an algorithm capable of solving problems with a single criterion.

The Enhanced GP-based PSO combines the cognitive components of the PSO, **pbest** and **gbest**, with the responses obtained from the GP, μ and σ. In the informative path planner, the ASVs are the particles, and the ASV fleet is represented by the swarm. The mean μ obtained from the GP represents the estimated model of the WQPs. The standard deviation σ is the uncertainty in the estimated model. The higher the value of the mean, the higher the level of water contamination.

During the monitoring task, water resource measurements are taken through the water quality sensors. It should be noted that all the ASVs have the same sensors. As a result, the fleet has a homogeneous capacity for measuring a WQP. These measurements $y_s(\mathbf{x})$, along with the coordinates that conform the $\mathcal{Q}$ set, are used to update the GP. After updating, the data from the maximum μ and σ values, along with the local best and global best values, are used to calculate the velocity $\mathbf{v}^{t+1}$

and the position $\mathbf{x}^{t+1}$ of each ASV p, Eq. 20.

$$\mathbf{v}_p^{t+1} = \omega \mathbf{v}_p^t + c_1 r_1^t[\mathbf{pbest}_p^t - \mathbf{x}_p^t] + c_2 r_2^t[\mathbf{gbest}^t - \mathbf{x}_p^t] + c_3 r_3^t[\mathbf{max\_un}^t - \mathbf{x}_p^t] + c_4 r_4^t[\mathbf{max\_con}^t - \mathbf{x}_p^t] \tag{20a}$$

$$\mathbf{x}_p^{t+1} = \mathbf{x}_p^t + \mathbf{v}_p^{t+1} \tag{20b}$$

The coordinates that are considered to obtain the best local **pbest** and global best **gbest** are the points where the ASVs have already passed. All these points form the set $\mathcal{U} \subset \mathcal{N}$. Within the set $\mathcal{U}$, there are the subsets $\mathcal{U}_{(p)}$, which are composed of the points through which each ASV p has traveled. Eq. 21a and Eq. 21b show how the values of local best and global best are obtained, respectively. The $\mathbf{max\_un}^t$ term is the coordinate where the maximum value of the model uncertainty (σ) is found at time t, Eq. 21c, and the $\mathbf{max\_con}^t$ term represents the coordinate where the maximum value of the model mean (μ) or maximum contamination value is obtained, Eq. 21d. The terms c_3 and c_4 are the acceleration coefficients that determine the significance of the uncertainty and contamination terms. r_3 and r_4 are random values that are within the range [0, 1].

$$\mathbf{pbest}_p^t = argmax\{\mu_s(\mathbf{x})\} : \mathbf{x} \in \mathcal{U}_{(p)} \tag{21a}$$

$$\mathbf{gbest}^t = argmax\{\mu_s(\mathbf{x})\} : \mathbf{x} \in \mathcal{U} \tag{21b}$$

$$\mathbf{max\_un}^t = argmax\{\sigma_s(\mathbf{x})\} : \mathbf{x} \in \mathcal{N} \tag{21c}$$

$$\mathbf{max\_con}^t = argmax\{\mu_s(\mathbf{x})\} : \mathbf{x} \in \mathcal{N} \tag{21d}$$

APPENDIX B
ACCELERATION COEFFICIENTS VALUES

The studies in [37] and [38] were conducted for fleets of 4 vehicles, which means that these values are not the optimal weights for other numbers of vehicles. Because of this, further studies are conducted to obtain the optimal values of the weights of the Enhanced GP-based PSO algorithm for exploration and exploitation approaches. The studies are performed with the same conditions mentioned in [37] and [38], using Bayesian optimization for the hyper-parameterization of the weights. The results obtained are shown in Table 9. When the number of vehicles is greater than 4, the weights do not have significant variations. Therefore, the weights of the Enhanced GP-based PSO terms for more than 4 vehicles are fixed to the values of the weights for 4 vehicles.

TABLE 9. Acceleration coefficients.

Coefficients		2 vehicles	3 vehicles	4 or more vehicles
Explore	c_1	0.2517	1.2131	2.0187
	c_2	3.4080	3.1476	0
	c_3	1.4596	1.5157	3.2697
	c_4	0	0	0
Exploit	c_1	2.7460	1.3588	3.6845
	c_2	3.3385	1.4528	1.5614
	c_3	0	0	0
	c_4	3	4	3.1262

ACKNOWLEDGMENT

This work has been partially funded by the Ministerio de Ciencia e Innovación under the Projects "AQUATRONIC (Ref. Codes: PID2021-126921OA-C22 and PID2021-126921OB-C21)" and "ECOPORT (Ref. Codes: TED2021-131326A-C22 and TED2021-131326B-C21)".

REFERENCES

[1] *Transforming Our World: The 2030 Agenda for Sustainable Development*, Dept. Econ. Social Affairs, United Nations, New York, NY, USA, 2016.

[2] M. Arzamendia, D. Gutierrez, S. Toral, D. Gregor, E. Asimakopoulou, and N. Bessis, "Intelligent online learning strategy for an autonomous surface vehicle in lake environments using evolutionary computation," *IEEE Intell. Transp. Syst. Mag.*, vol. 11, no. 4, pp. 110–125, Winter 2019.

[3] H. Duan, S. A. Loiselle, L. Zhu, L. Feng, Y. Zhang, and R. Ma, "Distribution and incidence of algal blooms in Lake Taihu," *Aquatic Sci.*, vol. 77, no. 1, pp. 9–16, Jan. 2015.

[4] H. Xu, H. W. Paerl, B. Qin, G. Zhu, and G. Gaoa, "Nitrogen and phosphorus inputs control phytoplankton growth in eutrophic Lake Taihu, China," *Limnol. Oceanogr.*, vol. 55, no. 1, pp. 420–432, Jan. 2010.

[5] A. M. Michalak et al., "Record-setting algal bloom in Lake Erie caused by agricultural and meteorological trends consistent with expected future conditions," *Proc. Nat. Acad. Sci. USA*, vol. 110, no. 16, pp. 6448–6452, 2013.

[6] F. Peralta, M. Arzamendia, D. Gregor, D. G. Reina, and S. Toral, "A comparison of local path planning techniques of autonomous surface vehicles for monitoring applications: The Ypacarai Lake case-study," *Sensors*, vol. 20, no. 5, p. 1488, Mar. 2020.

[7] S. Y. Luis, D. Gutiérrez-Reina, and S. T. Marín, "A dimensional comparison between evolutionary algorithm and deep reinforcement learning methodologies for autonomous surface vehicles with water quality sensors," *Sensors*, vol. 21, no. 8, p. 2862, Apr. 2021.

[8] F. P. Samaniego, "Intelligent online water quality monitoring through multiple autonomous surface vehicles using the Bayesian optimization framework," Ph.D. thesis, Universidad de Sevilla, Seville, Spain, 2022.

[9] W. Wei, Q. Ke, A. Zielonka, M. Pleszczynski, and M. Wozniak, "Vehicle parking navigation based on edge computing with diffusion model and information potential field," *IEEE Trans. Services Comput.*, early access, Jun. 30, 2023, doi: 10.1109/TSC.2023.3286332.

[10] M. Woźniak, A. Zielonka, and A. Sikora, "Driving support by type-2 fuzzy logic control model," *Expert Syst. Appl.*, vol. 207, Nov. 2022, Art. no. 117798.

[11] F. Peralta, D. G. Reina, and S. Toral, "Water quality online modeling using multi-objective and multi-agent Bayesian optimization with region partitioning," *Mechatronics*, vol. 91, May 2023, Art. no. 102953.

[12] Z. Peng, J. Wang, D. Wang, and Q.-L. Han, "An overview of recent advances in coordinated control of multiple autonomous surface vehicles," *IEEE Trans. Ind. Informat.*, vol. 17, no. 2, pp. 732–745, Feb. 2021.

[13] L. Bottarelli, M. Bicego, J. Blum, and A. Farinelli, "Orienteering-based informative path planning for environmental monitoring," *Eng. Appl. Artif. Intell.*, vol. 77, pp. 46–58, Jan. 2019.

[14] M. J. T. Kathen, I. J. Flores, and D. G. Reina, "An informative path planner for a swarm of ASVs based on an enhanced PSO with Gaussian surrogate model components intended for water monitoring applications," *Electronics*, vol. 10, no. 13, p. 1605, Jul. 2021.

[15] L. Jin, J. Rückin, S. H. Kiss, T. Vidal-Calleja, and M. Popovic, "Adaptive-resolution field mapping using Gaussian process fusion with integral kernels," *IEEE Robot. Autom. Lett.*, vol. 7, no. 3, pp. 7471–7478, Jul. 2022.

[16] G. Carazo-Barbero, E. Besada-Portas, J. L. Risco-Martín, and J. A. López-Orozco, "EA-based ASV trajectory planner for detecting cyanobacterial blooms in freshwater," in *Proc. Genetic Evol. Comput. Conf. (GECCO)*. New York, NY, USA: Association for Computing Machinery, 2023, pp. 1321–1329.

[17] E. Guerrero, F. Bonin-Font, and G. Oliver, "Adaptive visual information gathering for autonomous exploration of underwater environments," *IEEE Access*, vol. 9, pp. 136487–136506, 2021.

[18] J. Peterson, W. Li, B. Cesar-Tondreau, J. Bird, K. Kochersberger, W. Czaja, and M. McLean, "Experiments in unmanned aerial vehicle/unmanned ground vehicle radiation search," *J. Field Robot.*, vol. 36, no. 4, pp. 818–845, Jun. 2019.

[19] J. Chen, C. Du, Y. Zhang, P. Han, and W. Wei, "A clustering-based coverage path planning method for autonomous heterogeneous UAVs," *IEEE Trans. Intell. Transp. Syst.*, vol. 23, no. 12, pp. 25546–25556, Dec. 2022.
[20] J. Wang, Y. Liu, S. Niu, W. Jing, and H. Song, "Throughput optimization in heterogeneous swarms of unmanned aircraft systems for advanced aerial mobility," *IEEE Trans. Intell. Transp. Syst.*, vol. 23, no. 3, pp. 2752–2761, Mar. 2022.
[21] P. Zhang, C. Wang, N. Kumar, and L. Liu, "Space-air-ground integrated multi-domain network resource orchestration based on virtual network architecture: A DRL method," *IEEE Trans. Intell. Transp. Syst.*, vol. 23, no. 3, pp. 2798–2808, Mar. 2022.
[22] J. J. Acevedo, B. C. Arrue, I. Maza, and A. Ollero, "Distributed approach for coverage and patrolling missions with a team of heterogeneous aerial robots under communication constraints," *Int. J. Adv. Robotic Syst.*, vol. 10, no. 1, p. 28, Jan. 2013.
[23] J. Zhang, G. Han, J. Sha, Y. Qian, and J. Liu, "AUV-assisted subsea exploration method in 6G enabled deep ocean based on a cooperative Pac-Men mechanism," *IEEE Trans. Intell. Transp. Syst.*, vol. 23, no. 2, pp. 1649–1660, Feb. 2022.
[24] F. Peralta, D. G. Reina, S. Toral, M. Arzamendia, and D. Gregor, "A Bayesian optimization approach for multi-function estimation for environmental monitoring using an autonomous surface vehicle: Ypacarai Lake case study," *Electronics*, vol. 10, no. 8, p. 963, Apr. 2021.
[25] M. J. T. Kathen, P. Johnson, I. J. Flores, and D. G. Reina, "AquaFel-PSO: A monitoring system for water resources using autonomous surface vehicles based on multimodal PSO and federated learning," 2022, *arXiv:2211.15217*.
[26] M. Arzamendia, D. Gregor, D. G. Reina, and S. L. Toral, "An evolutionary approach to constrained path planning of an autonomous surface vehicle for maximizing the covered area of Ypacarai Lake," *Soft Comput.*, vol. 23, no. 5, pp. 1723–1734, Mar. 2019.
[27] M. Arzamendia, I. Espartza, D. G. Reina, S. L. Toral, and D. Gregor, "Comparison of Eulerian and Hamiltonian circuits for evolutionary-based path planning of an autonomous surface vehicle for monitoring Ypacarai Lake," *J. Ambient Intell. Humanized Comput.*, vol. 10, no. 4, pp. 1495–1507, Apr. 2019.
[28] C. Ke and H. Chen, "Cooperative path planning for air–sea heterogeneous unmanned vehicles using search-and-tracking mission," *Ocean Eng.*, vol. 262, Oct. 2022, Art. no. 112020.
[29] Y. Wang, P. Bai, X. Liang, W. Wang, J. Zhang, and Q. Fu, "Reconnaissance mission conducted by UAV swarms based on distributed PSO path planning algorithms," *IEEE Access*, vol. 7, pp. 105086–105099, 2019.
[30] Z. Zuo, X. Yang, Z. Li, Y. Wang, Q. Han, L. Wang, and X. Luo, "MPC-based cooperative control strategy of path planning and trajectory tracking for intelligent vehicles," *IEEE Trans. Intell. Vehicles*, vol. 6, no. 3, pp. 513–522, Sep. 2021.
[31] X. Zhang, S. Xia, X. Li, and T. Zhang, "Multi-objective particle swarm optimization with multi-mode collaboration based on reinforcement learning for path planning of unmanned air vehicles," *Knowl.-Based Syst.*, vol. 250, Aug. 2022, Art. no. 109075.
[32] J. Kennedy and R. Eberhart, "Particle swarm optimization," in *Proc. Int. Conf. Neural Netw. (ICNN)*, vol. 4, Aug. 1995, pp. 1942–1948.
[33] C. E. Rasmussen, "Gaussian processes in machine learning," in *Proc. Summer School Mach. Learn.* Berlin, Germany: Springer, 2003, pp. 63–71.
[34] D. E. Goldberg and J. H. Holland, "Genetic algorithms and machine learning," *Mach. Learn.*, vol. 3, nos. 2–3, pp. 95–99, 1988.
[35] M. Mitchell, *An Introduction to Genetic Algorithms*. Cambridge, MA, USA: MIT Press, 1998.
[36] K. De Jong, "Learning with genetic algorithms: An overview," *Mach. Learn.*, vol. 3, nos. 2–3, pp. 121–138, Oct. 1988.
[37] M. C. J. T. Kathen, I. J. Flores, and D. G. Reina, "A comparison of PSO-based informative path planners for autonomous surface vehicles for water resource monitoring," in *Proc. 7th Int. Conf. Mach. Learn. Technol. (ICMLT)*, Mar. 2022, pp. 271–276.
[38] M. J. Ten Kathen, D. G. Reina, and I. J. Flores, "A comparison of PSO-based informative path planners for detecting pollution peaks of the Ypacarai Lake with autonomous surface vehicles," in *Proc. Int. Conf. Optim. Learn. (OLA)*, 2022, pp. 1–3.
[39] F. P. Samaniego, D. G. Reina, S. L. T. Marín, M. Arzamendia, and D. O. Gregor, "A Bayesian optimization approach for water resources monitoring through an autonomous surface vehicle: The Ypacarai Lake case study," *IEEE Access*, vol. 9, pp. 9163–9179, 2021.
[40] A. Sakai, D. Ingram, J. Dinius, K. Chawla, A. Raffin, and A. Paques, "PythonRobotics: A Python code collection of robotics algorithms," 2018, *arXiv:1808.10703*.

MICAELA JARA TEN KATHEN was born in Ciudad del Este, Paraguay. She received the degree in electromechanical engineering from Universidad Católica "Nuestra Señora de la Asunción," Paraguay, in 2019. She is currently pursuing the Ph.D. degree in data sciences with Universidad Loyola Andalucía. She has been a Visitor Researcher with Liverpool John Moores University, U.K. She is a Research Assistant with Universidad Loyola Andalucía. She focuses her work on the development of monitoring systems for autonomous vehicles.

FEDERICO PERALTA SAMANIEGO was born in Asunción, Paraguay. He received the degree in mechatronics engineering from the National University of Asunción, Paraguay, in 2019, and the Ph.D. degree in automatics, electronics and telecommunications engineering from the University of Seville, in 2022. He is currently an Assistant Professor with Universidad Loyola Andalucía, Dos Hermanas, Spain. He focuses his work on the development of GNC systems for autonomous vehicles and robotics applications.

ISABEL JURADO FLORES received the degree (cum laude) in industrial engineering from the University of Seville, in 2007. She presented her Ph.D. thesis on control of communication network systems. She has carried out a research stay with The University of Newcastle, Australia. She is currently a Professor and a Researcher with Universidad Loyola Andalucía. Her research interests include control systems through communication networks, robust control, predictive control, and distributed systems.

DANIEL GUTIÉRREZ REINA received the B.E. degree (Hons.) in electronic engineering, the M.S. degree in electronics and telecommunications, and the Ph.D. degree (Hons.) in electronic engineering from the University of Seville, Seville, Spain, in 2009, 2011, and 2015, respectively. He was an Assistant Professor with Loyola University, from October 2018 to April 2019. He has been a Visitor Researcher with Liverpool John Moores University, U.K.; the Free University of Berlin, Germany; the Colorado School of Mines, USA; and Leeds Beckett University, U.K. He is currently an Associate Professor with Departamento de Ingeniería Electrónica, Universidad de Sevilla. He has published about 58 articles in JCR journals with impact factor. His current research interests include the application of meta-heuristic, machine learning, and deep algorithms to solve monitoring problems using autonomous systems. He is part of the editorial board of several journals, such as *International Journal of Distributed Sensor Networks* (SAGE), *Electronics* (MDPI), and *Future Internet* (MDPI), organizing numerous SI for these journals.